DESIGN OF A FRONT AERODYNAMIC BRAKE FOR AUTOMOBILES

In partial fulfillment of the requirements for the award of the degree of Bachelor of Technology
In
MECHANICAL ENGINEERING

BY
V N S CHANDAN (UG103252)
K SANTOSH PRAVEEN (UG103222)
V N V S SAI ARADH (UG103253)
SHINE EAPEN MATHAI (9394)

Under the guidance of

Dr. Y. RAVI KUMAR
Assistant Professor

DEPARTMENT OF MECHANICAL ENGINEERING
NATIONAL INSTITUTE OF TECHNOLOGY
WARANGAL-506004

2013-2014

DEPARTMENT OF MECHANICAL ENGINEERING
NATIONAL INSTITUTE OF TECHNOLOGY
WARANGAL – 506004

CERTIFICATE

This is to certify that the project entitled "**DESIGN of a FRONT AERODYNAMIC BRAKE FOR AUTOMOBILES**" carried out by V N S Chandan (UG103252),K Santosh Praveen (UG103222), V N V S Sai Aradh (UG103253), Shine Eapen Mathai (09394) of final year B.Tech Mechanical Engineering during academic year 2013-2014, is a bonafide work submitted to the National Institute of Technology, Warangal in partial fulfillment of requirements for the awards of the **Degree of Bachelor of Technology.**

_____	_____
Signature of project guide	Signature of Head of dept.
Dr. Y RAVI KUMAR	**Prof. L KRISHNANAND**
Assistant Professor	Head of Department
Mechanical Engineering Dept.	Mechanical Engineering Dept.
NIT Warangal.	NIT Warangal.

APPROVAL SHEET

This project entitled "**DESIGN OF A FRONT AERODYNAMIC BRAKE FOR AUTOMOBILES**" by V N S CHANDAN (UG103252), K SANTOSH PRAVEEN (UG103222), V N V S SAI ARADH (UG103253) and SHINE EAPEN MATHAI (09394) is approved for the **Bachelor of Technology (Mechanical Engineering).**

EXAMINERS

_____

_____

SUPERVISOR

_____

CHAIRMAN

_____

Date:_____

DECLARATION

We declare that this written submission represents our ideas in our own words and where others' ideas or words have been included, we have adequately cited and referenced the original sources. We also declare that we have adhered to all principles of academic honesty and integrity and have not misrepresented or fabricated or falsified any idea / data / fact / source in our submission. We understand that any violation of the above will be a cause for disciplinary action by the Institute and can also evoke penal action from the sources which have thus not been properly cited or from whom proper permission has not been taken when needed.

_____

V N S CHANDAN (UG103252)

_____

K SANTOSH PRAVEEN (UG103222)

_____

V N V S SAI ARADH (UG103253)

_____

SHINE EAPEN MATHAI (09394)

Date: _____

ACKNOWLEDGEMENTS

With great pleasure and deep gratitude, we take this opportunity to express our sense of indebtedness to **Dr. Y. Ravi Kumar**, Assistant Professor, Department of Mechanical Engineering, our project guide for accepting us under his good self to carry out this project work, and providing us his invaluable guidance and constant encouragement at each and every step throughout the course of this project.

We thank **Dr. Jayakrishna**, for assisting us to understand the Ansys Fluent software and helping us to further explore and utilize those features in our work.

We thank **Dr. V R K Raju**, who helped us in understanding the setting up of a wind tunnel. Without his guidance the experimental testing wouldn't have been a success.

We thank all the **staff workers** in the IC Engines Lab, who helped us in setting up and to carry out the experiments successfully.

We would also like to thank **Prof. L Krishnanand**, Head of Mechanical Department, National Institute of Technology, Warangal for giving us the opportunity to work on this project.

We would like to thank all the people we forgot to mention here and also to the sleepless night we spend.

V.N.S CHANDAN (UG103252)

K. SANTOSH PRAVEEN (UG103222)

V.N.V.S SAI ARADH (UG103253)

SHINE EAPEN MATHAI (09394)

ABSTRACT

According to recent statistics, the deaths caused by road accidents have increased over the years. The road fatalities per 100 000 motor vehicles in countries like US is 1600, in India is 900, UAE is 118.5. The major causalities are young adults. The one of the major factor for these accidents are over speeding, loss of vehicle control, brakes failure. This motivated us to explore the alternate option to increase the safety of passengers at the time of braking.

Brakes are used in cars to bring the vehicle to rest and to the safely maneuver the car. Also it increases the safety of the passengers. The control of vehicles at higher speeds has proved a tedious task to the engineers. Over the years the brakes have evolved for various applications. This led to the use of aerodynamics to brake the car.

Our project explores the aspect of aerodynamics in braking. This thesis deals with the design of front aerodynamic brake. The work started with the analysis of market available products for brakes and studied the various drawbacks of the products. The design was carried out on SolidWorks with various iterations leading to the final product shape. The simulation using Ansys Fluent software gave better results than any available standard product. The results obtained were tested for a passenger and sports car. The aerodynamic front brake was tested in wind tunnel which gave us satisfying results due to the unavoidable error. The brakes are actuated with the help of hydraulic actuators and levers. The deployment time for the brakes to come to the desired position is very minimal. From the results obtained from Ansys Fluent and Wind Tunnel, the thesis states that the drag coefficient has increased drastically which improves the braking force. An advantage of 60% increase in the drag is achieved. The future scope of the thesis is that it can be applied to other means of transport like fast moving trains and others. This aerodynamic front brake improves braking in other terrains like wet conditions and snow or general where there is less traction.

Further, keeping in mind the positive results, the team has decided to file for a patent on the brake.

CONTENTS

LIST OF FIGURES

LIST OF TABLES

CHAPTER 1

INTRODUCTION

In a little over a hundred years since the automobile took hold of people's imagination, technologies designed to make them accelerate faster and reach higher speeds have evolved with a fury the likes of which we can only see in the aeronautics industry. Still, despite chargers, turbochargers, twin turbochargers or NOX, there are limits which cannot be surpassed by a land based vehicle in terms of speed, be it because of technological limitations or the laws of physics.

Not the same can be said about the rather unseen part of the automotive evolution: brakes. The only limitations imposed to them are in connection with the human body's ability to withstand rapid decelerations. Otherwise, it would be a lot easier stopping a car than making it go insanely fast. Whether they come in the form of drum brakes, as was the case in the dawn of the automobile, or as discs, the brakes have been the horsepower's companion throughout the decades, each pulling the evolution of the car in different directions.[1]

1.1 Evolution of Brakes

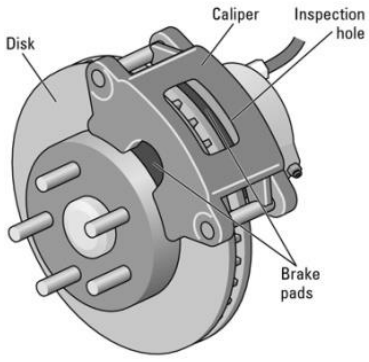

Fig. 1.1 Figure showingMechanical Disc Brake[2]

Fig. 1.2 Figure showing Mechanical Drum Brake [2]

At the most basic level, braking by friction involves pressing a stationary component against a rotating part until it stops turning. Over the years to keep things simple and cheap on the Model T, Henry Ford created an evolutionary dead-end with foot-operated cables that pulled on a belt wrapped around a drum in the transmission. Around the turn of the century, both disk and drum brake systems developed. Louis Renault went the latter route with asbestos-lined shoes pressing against the interior surface of a steel drum attached to the wheel. This basic design had an inherent performance advantage that has kept them in use more than a century later. The advent of electronics in the 1970s allowed engineers to insert a hydraulic control unit in between the brake pedal and the calipers or drums at each wheel, allowing those corners to be individually modulated based on signals from wheel speed sensors. Those first ABS systems have now been expanded to enable the systems to apply brakes autonomously of the driver to provide traction and stability control as well as automatic crash avoidance.[3]

1.1.1 Brake Material

With the evolution of high speed cars, braking systems had to keep up with the development under the hoods. This meant that regular gray iron brakes, albeit grooved, drilled and vented had to be replaced with more advanced technologies and even doubled by other speed disposal methods. The focus will be on the actual brakes, rather than on the control and assistance technologies. In the last 15 years or so, two main innovations have dramatically changed performance of automotive braking systems used on high-end series production cars. One being a material that made it all possible, carbon fiber reinforced carbon (carbon-carbon), formed by a graphite matrix reinforced with carbon fiber, was originally developed for intercontinental ballistic missiles. Thanks to its heat dissipating properties and great

performance to weight ratio, the carbon brake disc/caliper combination is the solution of choice for most elite motorsports on the globe. In an average race, an F1 car must decelerate from speeds exceeding 200 km/h (sometimes even 300 km/h) to about 70 km/h and it only has a few seconds to do so. This process can bring the brake rotor and pads up to 1000 °C and it is repeated about 800 times per race. So, the carbon-carbon brakes are not the perfect solution.[4]

A derivative material, carbon fiber-reinforced silicon carbide (C/SiC), a.k.a. carbon-ceramic, was used by British railway engineers in the late 80's. The wonder-child allowed road driving mortals to benefit from the new composite material's properties. First of all there is the carbon-ceramic disc/pads maximum allowed temperature of up to 1400 °C, offering a fade-free holy aura. The low thermal expansion of the material reduces juddering when the brakes are hot. Regular cast iron brake discs/pads also lose the battle in cold temperatures, as carbon-ceramic ones squeal and judder less at low temperatures. Then there's the weight advantage- the carbon brake discs are up to 60% lighter than the conventional cast iron ones, which reduces the overall and, maybe more importantly, un-sprung weight of the vehicle. Carbon-ceramic friction doesn’t create dust in the way that the steel one does, so fortunate owners won’t have to polish their rims so often. Last and maybe least, ceramic discs have a promised life span of up to 300,000 km, three or four time greater than cast iron ones.[4]

1.1.2 Aerodynamic Brakes

Another automotive deceleration technology apple which fell in the industry’s head is the aerodynamic brake. Alfred Neubauer, Mercedes’ director of motorsport at the time, came up in 1955 with the idea of equipping the 300 SLR race car with an aerodynamic brake. A hood placed behind the passenger(s) was lifted mechanically while braking, folding back after the brake pedal was released. The solution was implemented at that year’s Le Mans Race.[4]

Fig. 1.3 Figure showing deployed rear aerodynamic brake on Bugatti Veyron

The first road car featuring such a setup is the Bugatti Veyron, launched in 2005. In the first 0.4 seconds of any above 200 km/h Veyron braking process, the aero brake is automatically activated: the spoiler raises itself and makes a 55 degree angle with an imaginary horizontal line, reinforcing the car's carbon ceramic braking system 1.3 g deceleration with an additional 0.6 g.

However, its pure functional principle limits its road driving applicability. In other words it is only useful at very high speeds, the kind that even hypercar owners can find a bit difficult to maintain. Nevertheless, the aerodynamic brake remains much more exclusive than the carbon-ceramic one.[4]

1.2Rapid Prototyping

Rapid Prototyping (RP) can be defined as a group of techniques used to quickly fabricate a scale model of a part or assembly using three-dimensional computer aided design (CAD) data. The first methods for rapid prototyping became available in the late 1980s and were used to produce models and prototype parts. Today, they are used for a wide range of applicationsand are used to manufacture production-quality parts in relatively small numbers if desired without the typical unfavorable short-run economics. What is commonly considered to be the first RP technique, Stereo-lithography, was developed by 3D Systems of Valencia,

CA, USA. The company was founded in 1986, and since then, a number of different RP techniques have become available.[5]

In addition, RP models can be used for testing, such as when an airfoil shape is put into a wind tunnel. RP models can be used to create male models for tooling, such as silicone rubber molds and investment casts. In some cases, the RP part can be the final part, but typically the RP material is not strong or accurate enough. When the RP material is suitable, highly convoluted shapes (including parts nested within parts) can be produced because of the nature of RP.

Rapid Prototyping or manufacturing decreases development time by allowing corrections to a product to be made early in the process, mistakes can be corrected and changes can be made while they are still inexpensive. RP or RM can achieve extreme structural accuracy and is able to create almost any shape. The parts are first designed on a CAD (Computer Aided Design) system and then with the help of a 3D laser printing technology are being manufactured layer by layer until the model is completed from material in powder form.[5]

1.2.1 Process of creating models or final usable parts

Although several rapid prototyping techniques exist, all employ the same five-step process:

- Create a CAD model of desired part

Build the object using a Computer-Aided Design (CAD) software package. The designer can use a pre-existing CAD file or may wish to create one for prototyping purposes. This process is identical for all of the RP or RM building techniques.

- Convert the CAD model to .stl (stereolithography) computer format

The second step is to convert the CAD file into .stl format. The various CAD packages use a number of different algorithms to represent solid objects. To establish consistency, the .stl format has been adopted as the standard of the rapid prototyping industry. Since the .stl format is universal, this process is identical for all of the RP build techniques.

- Slice the .stl file into thin cross-sectional layers

In the third step, a pre-processing program prepares the .stl file to be built. Several programs are available, and most allow the user to adjust the size, location and orientation of the model. Build orientation is important for several reasons. First, properties of rapid prototypes vary from one coordinate direction to another. For example, prototypes are usually weaker and less accurate in the z (vertical) direction than in the x-y plane. In addition, part orientation partially determines the amount of time required to build the model. The pre-processing software slices the .stl model into a number of layers from 0.01 mm to 0.7 mm thick, depending on the build material. Each PR machine manufacturer supplies their own proprietary pre-processing software.

- Construct the model one layer atop another

The fourth step is the actual construction of the part. Using one of several techniques RP machines build one layer at a time from WINDFORM carbon fiber filled materials, polymers, plastic, paper, ceramic or powdered metal. Most machines are fairly autonomous, needing little human intervention.

- Clean and finish the model

The final step is actually post-processing. This involves removing the prototype from the machine and detaching any supports. Some photosensitive materials need to be fully cured before use. Manufactured parts may also require minor cleaning and surface treatment. Sanding, sealing, and painting the model will improve its appearance and durability.[6]

This technology has many different manufacturing processes.[7]

The main ones of these are:

- Stereo-lithography
- Solid Ground Curing
- Selective Laser Sintering
- Fused Deposition Modeling
- Laminated Object Manufacturing (LOM)
- Three Dimensional Printing (MIT) [7]

1.2.2 Fused Deposition Modeling

Fused deposition modeling (FDM) is an additive manufacturing technology commonly used for modeling, prototyping, and production applications.

FDM begins with a software process which processes an STL file (stereolithography file format), mathematically slicing and orienting the model for the build process. If required, support structures may be generated. The machine may dispense multiple materials to achieve different goals: For example, one may use one material to build up the model and use another as a soluble support structure, or one could use multiple colors of the same type of thermoplastic on the same model. The model or part is produced by extruding small beads of thermoplastic material to form layers as the material hardens immediately after extrusion from the nozzle. A plastic filament or metal wire is unwound from a coil and supplies material to an extrusion nozzle which can turn the flow on and off. There is typically a worm-drive that pushes the filament into the nozzle at a controlled rate. The nozzle is heated to melt the material. The thermoplastics are heated past their glass transition temperature and are then deposited by an extrusion head. The nozzle can be moved in both horizontal and vertical directions by a numerically controlled mechanism. The nozzle follows a tool-path controlled by a computer-aided manufacturing (CAM) software package, and the part is built from the bottom up, one layer at a time. Stepper motors or servo motors are typically employed to move the extrusion head. [8]

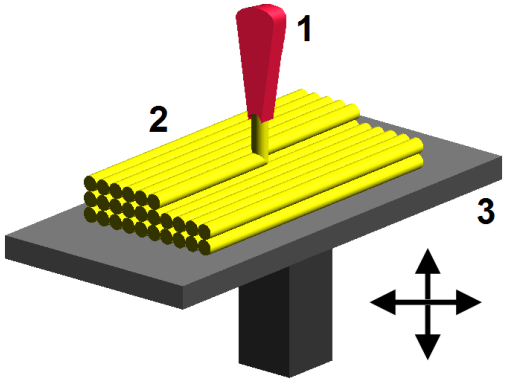

Fig. 1.5 Figure showing the layer-by-layer FDM process[8]

Although as a printing technology FDM is very flexible, and it is capable of dealing with small overhangs by the support from lower layers, FDM generally has some restrictions on the slope of the overhang, and cannot produce unsupported stalactites. FDM uses the thermoplastics ABS, ABSi, polyphenylsulfone (PPSF), polycarbonate (PC), and Ultem 9085,

among others. These materials are used for their heat resistance properties. Ultem 9085 also exhibits fire retardancy making it suitable for aerospace and aviation applications. FDM is also used in prototyping scaffolds for medical tissue engineering applications

1.2.3 Rapid Prototyping Machine

Specifications:

Table.1.1. Specifications of the Rapid Prototyping Machine

Model	Dimension SST 768.
Make	Stratasys, USA
Build Volume	254*254*305 mm
Material	ABS Plastic
Form of material	Filament on spool
Support removal	Soluble Support technology
Software	Catalyst® EX
Network Connectivity	TCP/IP 100/10 base T
Workstation Compatibility	Windows XP
Layer Thickness	0.254 mm (or) 0.33 mm
Energy source	Heated extrusion tip
Size of the Machine	914*686*1041 mm
Weight of the Machine	128 kg
Power requirements	110-120 VAC, 60 Hz, 15A

Fig. 1.6 Figure showing the Rapid Prototyping Machine

1.3Wind Tunnel

Wind tunnel is structure used for studying the interaction between a solid or gel bodies and airstreams. A wind tunnel simulates interaction by producing a high-speed airstreams which flow passing a model being tested. The model is fixed inside testing area of the tunnel so that lift and drag forces on it can be measured by measuring the tensions on the fixing structure.[9]

Wind tunnels may be classified according to their basic architecture (open-circuit, closed-circuit), according to their speed (subsonic, transonic, supersonic, hypersonic), according to the air pressure (atmospheric, variable- density), or their size (ordinary scaled or full-scale). There are a number of wind tunnels (meteorological tunnel called also Boundary layer tunnel, shock tunnel, plasma-jet tunnel, hot-shot tunnel) that fall in a special category of their own. In F1, pressurized wind tunnels are not allowed by FIA rules.

In wind tunnels operating well below the speed of sound, the airstream is created by large motor-driven fans. At velocities near or above the speed of sound, the airstream is created either by releasing highly compressed air from a tank at the upwind end of the tunnel testing area, or by allowing air to rush through the tunnel into a previously created vacuum tank at its downwind end. Sometimes these methods are combined, especially for the production of hypersonic velocities, i.e., velocities at least five times as great as the speed of sound. [9]

Main components of a tunnel are: Entrance cone, test section, regain passage, propeller/motor, and return passage. Flow straighteners, corner vanes, honeycomb layers for reduced turbulence, air heat exchangers and diffusers are other common features. Pressures on the model surface are measured through small flush openings in its surface or with pitot tubes fitted on surface of tested object. Forces exerted on the model may be determined from measurement of the airflow upstream and downstream of the model. Most automobiles produce lift. As the speed increases, the lift force increases and the car becomes unstable. In order to counteract this problem, modern race cars are designed to produce negative lift. The typical family sedan has a lift coefficient of about 0.3, while a F1 car can have a lift coefficient of 3.80. You can easily see the significant amount of downforce that a race car can produce. All of these things are easy observed, tested and modified in wind tunnel in controlled space with controlled air temperature and pressure, in controlled speed without actually driving the car. [9]

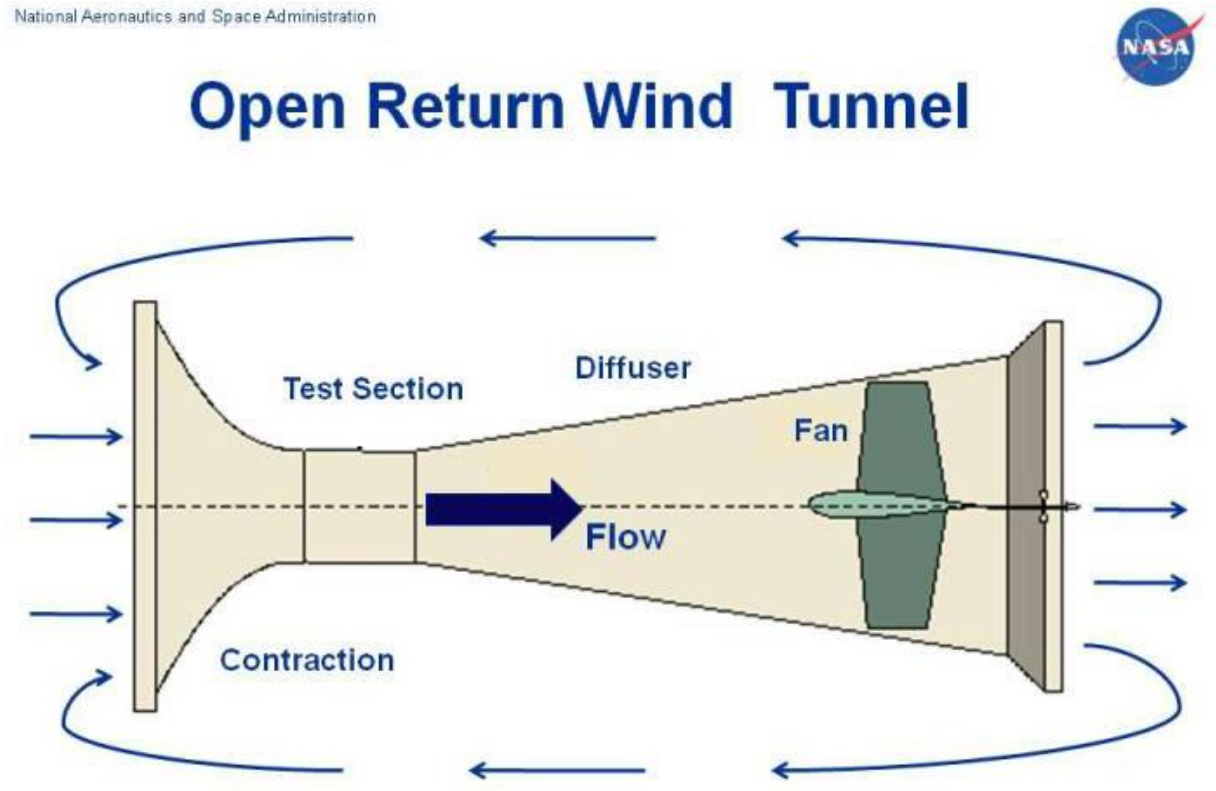

Fig. 1.7 Figure showing the schematic of an Open return wind tunnel[10]

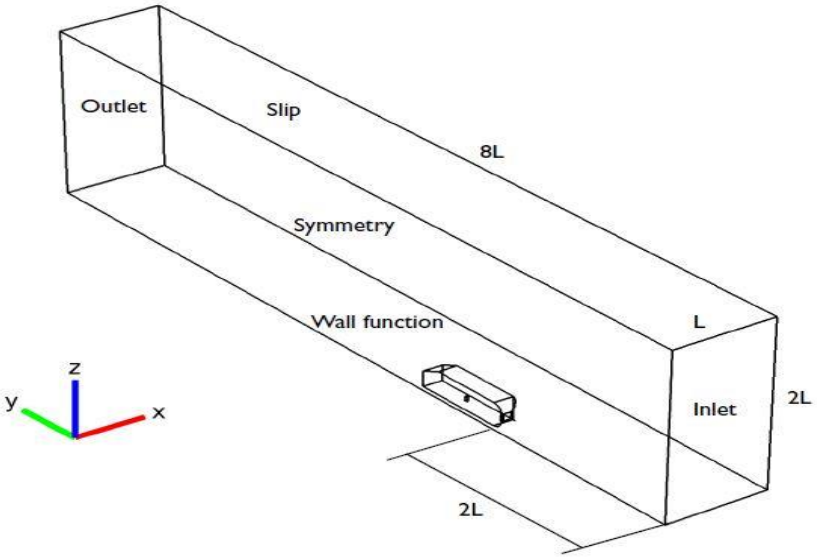

Fig. 1.8 Figure of an Ahmed Body inside a Wind tunnel setup

CHAPTER 2

LITERATURE REVIEW

2.1 Turbulent Flow

A turbulent flow field is characterized by velocity fluctuations in all directions and has an infinite number of scales (degrees of freedom). Solving the NS equations for a turbulent flow is impossible because the equations are elliptic, non-linear, coupled (pressure-velocity, temperature-velocity). The flow is three dimensional, chaotic, diffusive, dissipative, and intermittent. The most important characteristic of a turbulent flow is the infinite number of scales so that a full numerical resolution of the flow requires the construction of a grid with a number of nodes that is proportional to $Re^{9/4}$. [11]

The turbulent models are as follows[11], in order of increasing complexity:

- Algebraic (zero equation) models : mixing length (first order model)
- One equation models: k-model, μ_t-model (first order model)
- Two equation models : k-ε, k-kl, k-w^2, low R_e k-ε (first order model)
- Algebraic stress models : ASM (second order model)
- Reynolds stress model : RSM (second order model)

K-epsilon (k-ε) turbulence model is the most common model used in Computational Fluid Dynamics (CFD) to simulate turbulent conditions. It is a two equation model which gives a general description of turbulence by means of two transport equations (PDEs). The original impetus for the K-epsilon model was to improve the mixing-length model, as well as to find an alternative to algebraically prescribing turbulent length scales in moderate to high complexity flows. The first transported variable determines the energy in the turbulence and is called turbulent kinetic energy (k). The second transported variable is the turbulent dissipation (epsilon) which determines the rate of dissipation of the turbulent kinetic energy.[12]

The k-ε model has been tailored specifically for planar shear layers and recirculation flows. This model is the most widely used and validated turbulence model with applications ranging from industrial to environmental flows, which explains its popularity. It is usually useful for free-shear layer flows with relatively small pressure gradients as well as in confined

flows where the Reynolds shear stresses are most important. It can also be stated as the simplest turbulence model for which only initial and/or boundary conditions needs to be supplied. However it is more expensive in terms of memory than the mixing length model as it requires two extra PDEs.[12] This model would be an inappropriate choice for problems such as inlets and compressors as accuracy has been shown experimentally to be reduced for flows containing large adverse pressure gradients. The k-ε model also performs poorly in a variety of important cases such as unconfined flows, curved boundary layers, rotating flows and flows in non-circular ducts.

2.2 Bluff body

Bluff bodies refer to bodies with blunt bases that cause leading-edge flow separation and the formation of recirculation regions in the near wake of the bluff body[14]. This results in a lower pressure on the back surface of the body and sets up a large difference between the relatively high pressure acting on the front of the bluff body and the lower base pressure. Automotive bodies are considered as bluff bodies moving in close proximity to the ground. It has been established that the pressure drag is a direct consequence of flow separation which occurs primarily at the rear end of the body[15]. More recently, Morelli (2000)[16] mentioned that pressure drag can contribute to approximately 75% to 85 % of total drag.

2.3 Ahmed body

The Ahmed body represents a simplified, ground vehicle geometry of a bluff body. Its shape is simple enough to allow for accurate flow simulation but retains some important practical features relevant to automobile bodies. The geometry was first defined by Ahmed, who also measured its aerodynamic properties in wind-tunnel experiments.

The important features of flow around a bluff body are the regions of flow separation and recirculation in the wake and even the simple shapes produce complex flow structures. These structures are formed in the vehicle wake, which is the main flow separation region, governing the drag experienced by the body [17]. To achieve the qualitative understanding of the relation between wake structure, pressure distribution, drag and geometric configuration [15], proposed a simplified car model which could generate main flow features of real vehicles without their geometric details. The simplified car model consists of three parts; fore body, mid-section and rear body. The edges of the fore body are rounded to avoid flow

separation. The midsection is a rectangle with sharp edges. The rear end has interchangeable geometry which can be used to study the effect of different geometric configurations on aerodynamic drag and pressure distribution. In the experiments conducted by Ahmed et al. (1984) [15], nine interchangeable rear bodies with different base slants from 0^0 to 40^0 were tested.

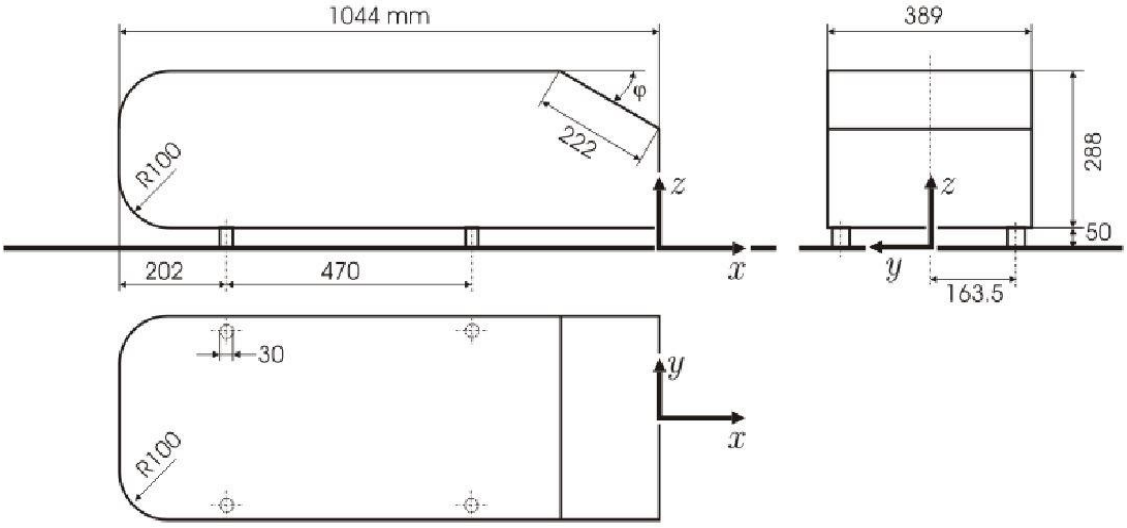

Fig. 1.4 Figure showing the dimensions of the standard Ahmed Body

The Ahmed body is presented in Figure 1.4. The total length (L) of the body is 1.044 m from front to end. It is 0.288 m in height and 0.389 m in width. Cylindrical legs 0.05 m in length are attached to the bottom surface. The angle of the rear slanting surface is typically varied between 0 and 40 degrees. This particular geometry has a slant angle of 25 degrees.[13]

2.4 Effect of Reynolds number on Drag Coefficient [13]

The experiments conducted by Ahmed et al. (1984) were performed at a wind speed of 60 m/s. This corresponds to a Reynolds number of 4.29 million based on model length. Bayraktar (2001) studied the effect of Reynolds number on lift and drag coefficients. The experiments were performed at Reynolds number in the range of 2.2 to 13.2 million. It was observed that over this wide range of Reynolds number, the drag coefficient only altered by 3.5 percent while the lift coefficient altered by 2 percent. Thus it was concluded that the drag coefficient is insensitive at high Reynolds numbers (of the order of 106).The experiments conducted by Ahmed et al. (1984) were performed at a wind speed of 60 m/s. This corresponds to a Reynolds number of 4.29 million based on model length. Bayraktar (2001)[18] studied the

effect of Reynolds number on lift and drag coefficients. The experiments were performed at Reynolds number in the range of 2.2 to 13.2 million. It was observed that over this wide range of Reynolds number, the drag coefficient only altered by 3.5 percent while the lift coefficient altered by 2 percent. Thus it was concluded that the drag coefficient is insensitive at high Reynolds numbers (of the order of 106).

2.5 Alterations of Formula 3 Race Car Diffuser Geometry for Optimized Down force

The Author deals with the aerodynamic behavior and performance of a Formula-3 Race car diffuser. The effects of operating parameters such as ride height, diffuser length and ramp angle on down-force along the straights are dealt. Even one-hundredth of a second matters a lot in Motor Racing. The Diffuser being an under-body aerodynamic component plays a vital role in enabling the car to carry speed on Track. Overtaking is an important aspect of Racing, as it helps in gaining track position and ultimately the race finish order. Hence, the above mentioned parameters are taken into consideration and its set-up changes are closely examined to improve overtaking maneuverability. Steady state conditions have been considered with the analysis of flow around a bluff body configuration due to the complexity of a complete Formula 3 car. Computational Analysis performed on a bluff body subjected to 3-D axial flow is completed using ANSYS Fluent package.[19]

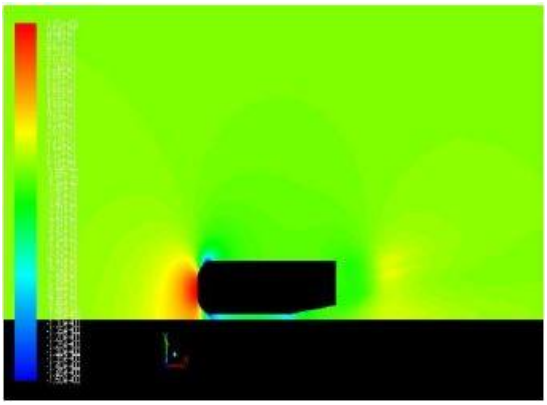

Fig. 2.1 Pressure plot at 8^0

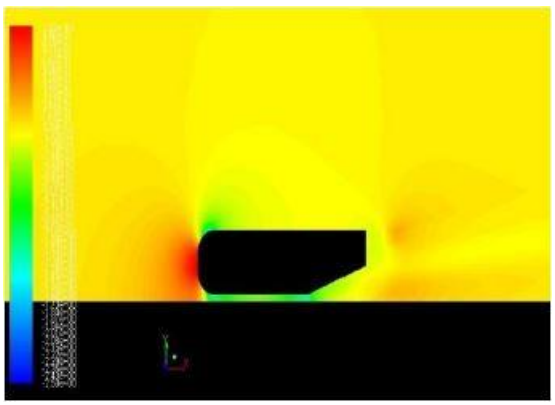

Fig. 2.2: Pressure plot at 20^0

2.6 Application of Rapid Prototyping Methods to High-Speed Wind Tunnel Testing

The author deals with the suitability of models constructed using rapid prototyping (RP) methods for use in subsonic, transonic, and supersonic wind tunnel testing and if these models meet the structural requirements of subsonic, transonic, and supersonic testing while still having the high fidelity required to produce accurate aerodynamic data.[20]

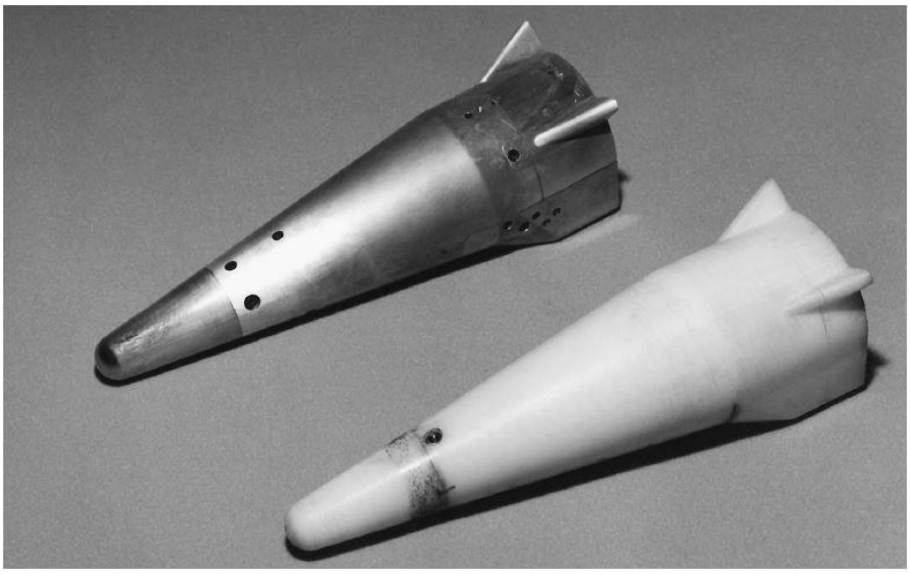

Fig 2.3 Photograph of both steel and FDM–ABS Vertical Lander configurations.

The study involved the construction of a fused deposition model to replicate the geometry of a model already slated for testing in the Marshall Space Light Center's (MSFC's) 14-Inch Transonic Wind Tunnel (TWT). This allowed a brief 20-run study which provided the necessary data to compare the aerodynamic characteristics of an RP model to that of a standard steel machined model. The findings from this initial study indicated that the aerodynamic database obtained from RP models showed good agreement with data obtained from the machined steel counterpart. This warranted a more complete study using the various rapid prototyping methods against a more intricate model.

CHAPTER 3

PROBLEM STATEMENT

The aim of the project is to design an aerodynamic brake especially for fast cars. When these cars brake at high speeds, say in the excess of 140 kmph, a flat plate is deployed from the roof of the car. Logic dictates that the flat plate will disturb the flow over the car and create a large wake thus increasing the drag force acting on the car. This increase in drag force is necessary so as to decrease the braking time and braking distance. And this will also aid in reducing the temperatures reached at the mechanical brakes, increasing the durability of the brakes and reliability.

Though qualitatively speaking, this brake will increase the drag, but the effectiveness in terms of change in coefficient of drag should be observed. For this, the Ahmed body is to be physically modeled on simulation software like ANSYS Fluent V14.5 with and without the flat plate and the results are to be observed.

Further, in an attempt to validate the result experimentally, the Ahmed body will be subjected to wind-tunnel testing using a sub-sonic wind tunnel.The test body will be manufactured in a Rapid prototyping machine. Since the flat plate requires some deploying mechanism, the actuation requirements of the brake will also be dealt with.

Lastly, the effect of the aerodynamic brake will be observed on a 2D model of a road car in order to establish its effectiveness.

CHAPTER 4

METHODOLOGY

The problem was planned to be tackled using experimental and numerical techniques. Since the problem is too complicated, writing a code was deemed highly unfeasible. Hence ANSYS Fluent Version 14.5 was used for simulation. And for experimental analysis, a sub-sonic wind tunnel running at a constant speed of 160 kmph(44.44 m/s) was used. An appropriately scaled RP model of Ahmed body was used as the test subject.

The procedure for both the methods is explained in detailed way below:

4.1 PHYSICAL MODELLING USING ANSYS FLUENT

Before the results of any parametric studies on Fluent can be justified, theprocedure must first be validated. If the obtained Coefficient of drag was found to match with the benchmark values, the procedure is said to be validated. But the procedure followed both for validation and parametric studies is the same.

4.1.1Geometry

(i)Fluent was used to simulate the flow over the Ahmed body in a wind tunnel with and without the aerodynamic brake plate.

(ii)Firstly, the Ahmed Body was modeled in SOLIDWORKS 14.For the model to be exported to ANSYS Fluent, it was saved as an ".iges" file.

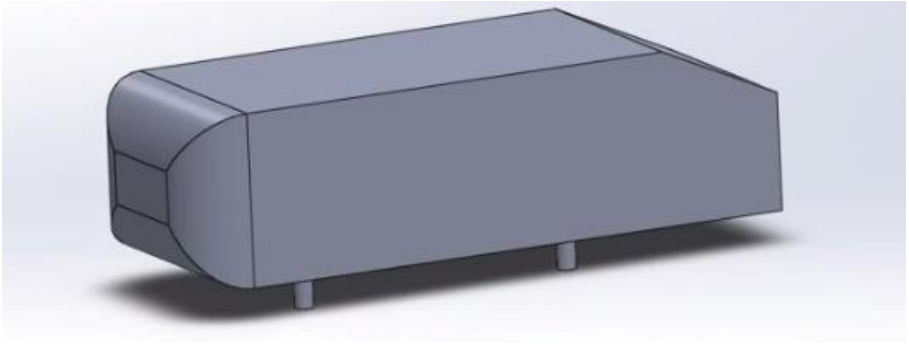

Fig. 4.1 Ahmed Body

(iii)ANSYS WORKBENCH was opened and fluent tab was selected from the list of options on the right.

(iv)The geometry was imported to Fluent by selecting the “Import Geometry” option. In the next step, the geometry modeler was started so as to edit the geometry.

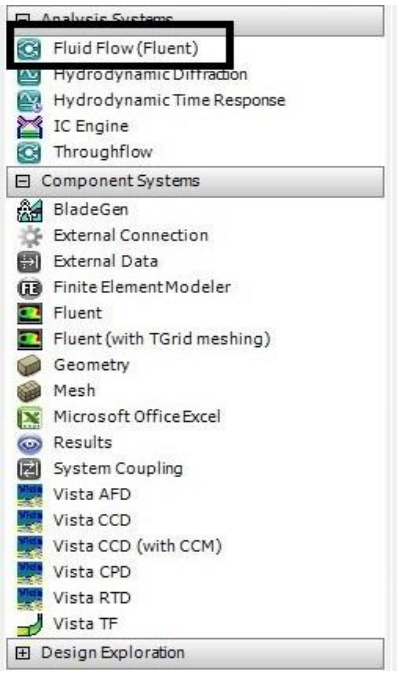

Fig. 4.2 List of options

(v)Once the Geometry Modeler was started, the body was frozen. The reason for that will be stated in the subsequent steps.

(vi)The next step is to create an enclosure around the Ahmed body.

(vii)The dimensions of the enclosure were chosen in such a way that the walls of the enclosure will have negligible effect on the solution of the problem. As suggested by literature, the length between the inlet and the body, the top and the body, the side and the body was chosen to be equal to three times the car length which is approximately about 3000 mother length between the outlet and the body was chosen to be 5 times the car length, which was about 5000 mm.

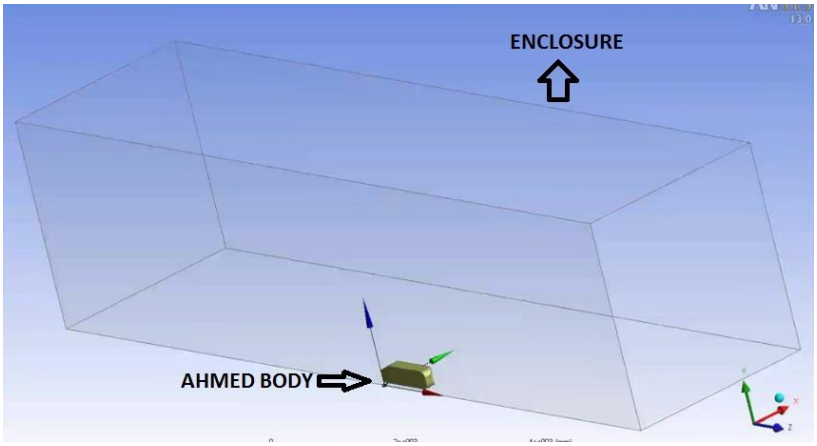

Fig. 4.3 Enclosure

(vii)Since the body is symmetric about its central plane, only one half of the body was modeled so as to decrease the computational time.

(viii)The body now was subtracted from the enclosure using the “Boolean” tool and “Subtract” option. This finished the geometric modeling of the problem.

4.1.2Meshing

Meshing is probably the most crucial in the physical modeling of any fluid flow problem. The steps followed are as follows:

(i)Initially, a first guess was done so as to get a “pilot” version of the mesh. The obtained was deemed to be too coarse

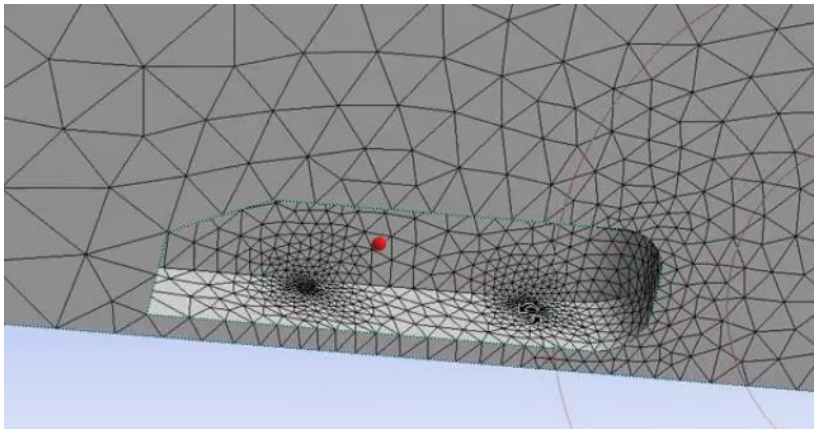

Fig. 4.4 Meshing

(ii)The following changes were brought out in the parameters of the mesh:

(a) Sizing

- The sizing function was changed from “Curvature” to “Proximity and Curvature” so that mesh varies with proximity as well.
- The span angle center was made fine so that more detail that more detail could be captured.
- The curvature angle was changed to 18^0
- The minimum size of the mesh was changed to 18mm so that a finer mesh could be obtained.
- Others were left as default.

(b) Inflation Layer

- The basic use of an inflation layer in meshing is to capture the boundary effects more properly. The following changes were made:
- The “Program Controlled Inflation Layer” option was chosen so that Fluent itself defines best possible inflation layer
- The “First Aspect ratio” type inflation layer was chosen so that we’ll have a finer mesh near the body and it becomes coarser as we move away from the body.

(c) Face sizing functions

- A face sizing functions was introduced all over the 9 faces of the Ahmedbody. Further the minimum mesh size was changed to 10 mm.

(ii)The whole mesh was then updated.

(iii) Named Selections were so that the definition of boundary conditions could be easily done.

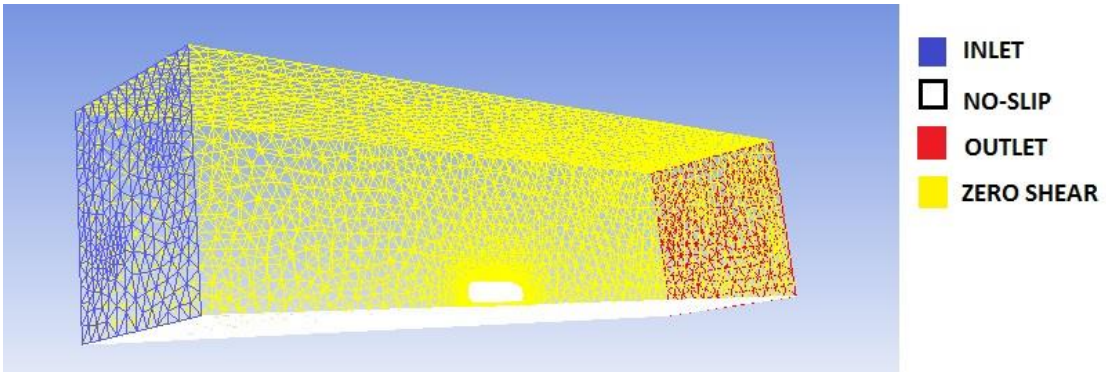

Fig. 4.5 Enclosure Boundaries

(iv)Since there is a separation of flow behind the car, a car box was introduced which had dimensions larger than the Ahmed body.The element size was reduced to 10mm

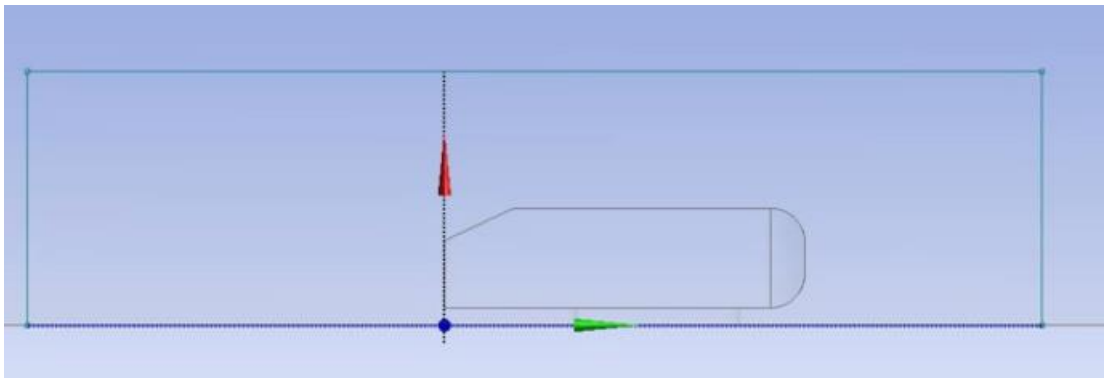

Fig. 4.6 Car box geometry

(v)The mesh was updated and this finished the meshing process.

(vi)The progress was saved.

4.1.3Setup

(i)The Fluent tab in the Workbench was opened.

(ii)Since the flow is highly turbulent, a proper turbulent model was to be chosen. Literature suggests that for flows with small pressure gradients like flow over aero foils, cars etc. k-epsilon is good enough. Literature also suggests that “Realizable k-epsilon” with “Non-equilibrium Wall functions” is best suited for car aerodynamics, the same model was chosen.

(iii)The next step is the definition of Boundary Conditions. The conditions were as follows:

- INLET

  A velocity of 40 m/s normal to the inlet was chosen. A turbulence intensity of 1% and turbulent viscosity ratio of 10 was used.

Figure 4.7 Figure showing the Panel for selection

- AHMED BODY

  The boundary condition applied here is the No-slip condition.
- WALLS

  The Boundary condition applied here is the zero shear condition.
- ROAD

  The boundary condition used here was the no-slip condition.
- OUTLET

  The boundary condition used here was “pressure outlet”. Aturbulence intensity of 5% and a turbulent viscosity ratio of 10 were used.
- SYMMETRY

  Along the symmetry plane, a zero shear condition was used.

(iv)The next was to choose the solution methods. “Coupled” scheme was chosen. It must be noted that the results obtained with “SIMPLE” scheme were almost the same. All the variables were approximated as a first order difference. After that, they were approximated as a second order till the solution converged.

(v)For a proper engineering solution, a residual of 0.0001 was selected. The percentage error in such a case was about 0.01% which is acceptable.

(vi)To study the variation of drag coefficient with each iteration, a drag monitor was setup.

(vii)The solution was initialized and was to run till it converged.The solution generally converged in about 550-600 iterations.

(vii)Necessary graphics like velocity, pressure contours along the symmetry plane were setup.

(viii)The results obtained were in good agreement with the benchmark values,the procedure was validated.

4.1.4 Parametric Studies

(i)To decide the height, angle of inclination and position of the brake plate, parametric studies were decided to best approach. Two parameters were kept constant and other one varied. This was done for all the three parameters.

(ii)Results were established and conclusions were drawn.

4.2 WIND TUNNEL TESTING

Literature suggests that experimental validation of any problem is the best. Hence it was the wind tunnel testing the Ahmed body with and without the brake plate was done.The test body was manufactured using a Rapid Prototyping Machine. Due to manufacturing limitations of the RP machine, a one-fifth scale model was used.

Fig.4.8 Wind Tunnel Testing facility

To find out the pressure distributions over the body, copper tubes were used. Holes were drilled through the top and bottom surfaces. The copper tubes were placed so that there was minimum flow disturbance. Further, two tube tips, one each at the front and rear ends were fixed. These copper tube ends were connected to a multi-tube manometer through flexi pipes, to measure the pressure at various points. Calculations were made based on the obtained results.

Fig. 4.9 Multi-tube Manometer

Fig. 4.10 Ahmed body showing Pressure taping

Fig. 4.11 Pressure tapings on the Ahmed body

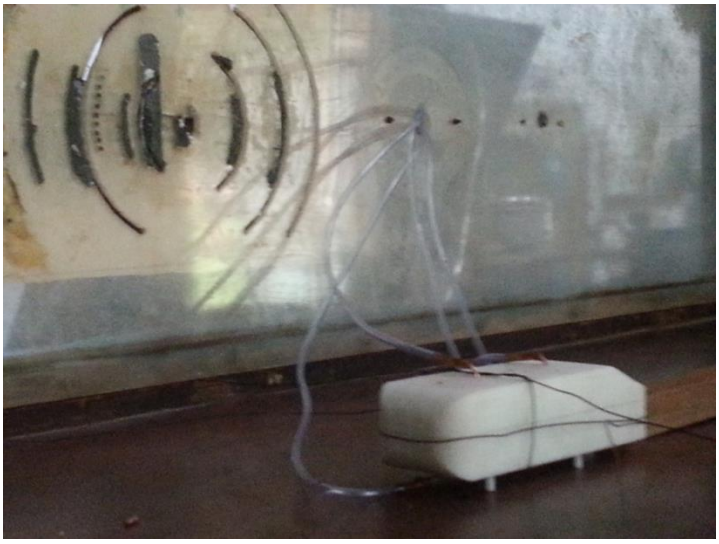

Fig.4.12 Flexi tubes used to connect the pressure tappings and manometer

4.3. EFFECTIVENESS TEST ON A ROAD CAR

Since an Ahmed body is not a road car, the effectiveness of the brake was observed on a road car. Due to size constraints on the Rapid Prototyping Machine and RAM limitations on using a 3D model, it was decided to simulate a 2D road car. Logically speaking, the drag coefficient of the 2D model will be less due to absence of induced drag at the sides.

The simulations are with certain assumptions:

(i)A 2D model is used.

(ii)The friction factor between the road and the car is 0.5

(iii)The drag coefficient remains more or less constant.

(iv)The tires are completely removed in order to avoid an error due to the formation of "non-manifold bodies".

The specifications of the car are:

Width: 1998 mm

Height: 1204 mm

Weight: 1800 kg

Height of brake plate =300 mm

Angle of inclination: 55^0

CHAPTER 5

ACTUATORS

An actuator is a type of motor that is responsible for moving or controlling a mechanism or system. It is operated by a source of energy, typically electric current, hydraulic fluid pressure, or pneumatic pressure, and converts that energy into motion. An actuator is the mechanism by which a control system acts upon an environment. The control system can be simple (a fixed mechanical or electronic system), software-based (e.g. a printer driver, robot control system), a human, or any other input.

In a modem car more than 100 actuators are used to control engine, transmission and suspension performance, to improve safety and reliability and enhance driver comfort. Most of these actuators today are electric motors, solenoids, thermo bimetals, wax motors, vacuum or pressure actuators.

5.1 Types of Actuators

The different types of actuators are

- Hydraulic
- Pneumatic
- Electrical
- Mechanical

5.1.1 Hydraulic Actuators

A hydraulic actuator consists of a cylinder or fluid motor that uses hydraulic power to facilitate mechanical operation. The mechanical motion gives an output in terms of linear, rotary or oscillatory motion. Because liquid is nearly incompressible, a hydraulic actuator can exert considerable force, but is limited in acceleration and speed.

The hydraulic cylinder consists of a hollow cylindrical tube along which a piston can slide. The term double acting is used when pressure is applied on each side of the piston. A difference in pressure between the two side of the piston results in motion of piston to either side. The term single acting is used when the fluid pressure is applied to just one side of the

piston. The piston can move in only one direction, a spring being frequently used to give the piston a return stroke.

5.1.2 Pneumatic Actuators

A pneumatic actuator converts energy formed by compressed air at high pressure into either linear or rotary motion. Pneumatic energy is desirable for main engine controls because it can quickly respond in starting and stopping as the power source does not need to be stored in reserve for operation.

Pneumatic actuators enable large forces to be produced from relatively small pressure changes. These forces are often used with valves to move diaphragms and so affect the flow of liquid through the valve.

5.1.3 Electric Actuators

An electric actuator is powered by a motor that converts electrical energy to mechanical torque. The electrical energy is used to actuate equipment such as multi-turn valves. It is one of the cleanest and most readily available forms of actuator because it does not involve oil.

5.1.4 Mechanical Actuators

A mechanical actuator functions by converting rotary motion into linear motion to execute movement. It involves gears, rails, pulleys, chains and other devices to operate. An example is a rack and pinion.

Examples of actuators used in Automobiles

- Electric Motor
- Pneumatic Actuator
- Hydraulic Piston
- Relay
- Comb Drive
- Piezoelectric Actuator
- Thermal Bimorph

5.2 Performance Metrics [21]

Performance metrics for actuators include speed, acceleration, and force (alternatively, angular speed, angular acceleration, and torque), as well as energy efficiency and considerations such as mass, volume, operating conditions, and durability, among others.

Force:

When considering force in actuators for applications, two main metrics should be considered. These two are static and dynamic loads. Static load is the force capability of the actuator while not in motion. Conversely, the dynamic load of the actuator is the force capability while in motion. The two aspects are rarely have the weight capability and must be considered separately.

Speed:

Speed should be considered primarily at a no-load pace, since the speed will invariably decrease as the load amount increases. The rate the speed will decrease will directly correlate with the amount of force and the initial speed.

Operating Conditions:

Actuators are commonly rated using the standard IP rating system. Those that are rated for dangerous environments will have a higher IP rating than those for personal or common industrial use.

Durability:

This will be determined by each individual manufacturer, depending on usage and quality.[21]

5.3 Working Principle

The actuator system consists of mainly hydraulic actuator, levers, and the brake plate.

Once the speed crosses over 120 kmph the speedometers sends a signal to the Electronic Control Unit (ECU). The ECU sends the signal to the hydraulic actuators to come to the initial position. Once the brakes are applied the ECU sends the signal to the actuators to

activate the brake plate. The brake plate comes to the maximum position thereby by providing the drag. When the brakes are released the ECU sends the signal to bring the brake plate back to the initial position.

The block diagram of actuators working:

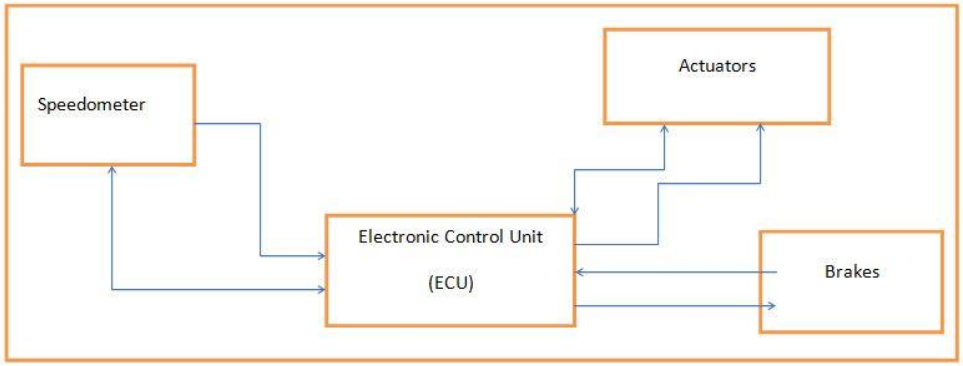

Fig.5.1 Block diagram showing how actuators work

The figure given below explains the working in a pictorial manner.

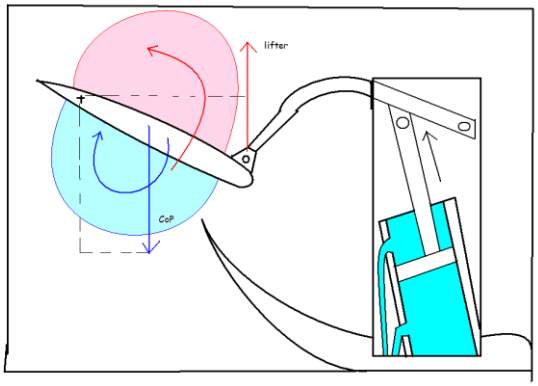

Fig.5.2 Working of brake plate using actuators

CHAPTER 6

RESULTS

The results observed have been divided into three sections; they are the results from validation, the results from parametric studies and the results from the wind tunnel testing.

6.1 VALIDATION

Parameters:

Length: 1044 mm

Kinematic viscosity: $15.68*10^{-6}$ m^2/s

Velocity: 40 m/s

Reynolds number= 2,561,224.488 ~ $2.5*10^6$

The above Reynolds number suggests the flow is highly turbulent.

Table.6.1. Comparison of results of benchmark with obtained values.

C_d Actual	C_d Obtained	Error %
0.2600	0.2716	4.4

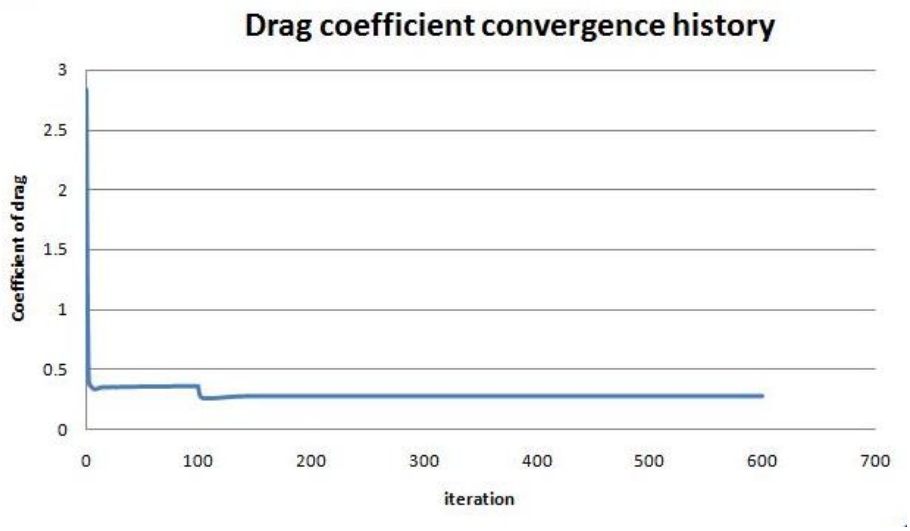

Fig. 6.1 Graph showing Drag coefficient convergence

6.2 PARAMETRIC STUDIES

(i)Without the brake plate

As already shown above, the coefficient of drag is 0.2716.

The velocity contour of the Ahmed body obtained in as in Fig.5.2

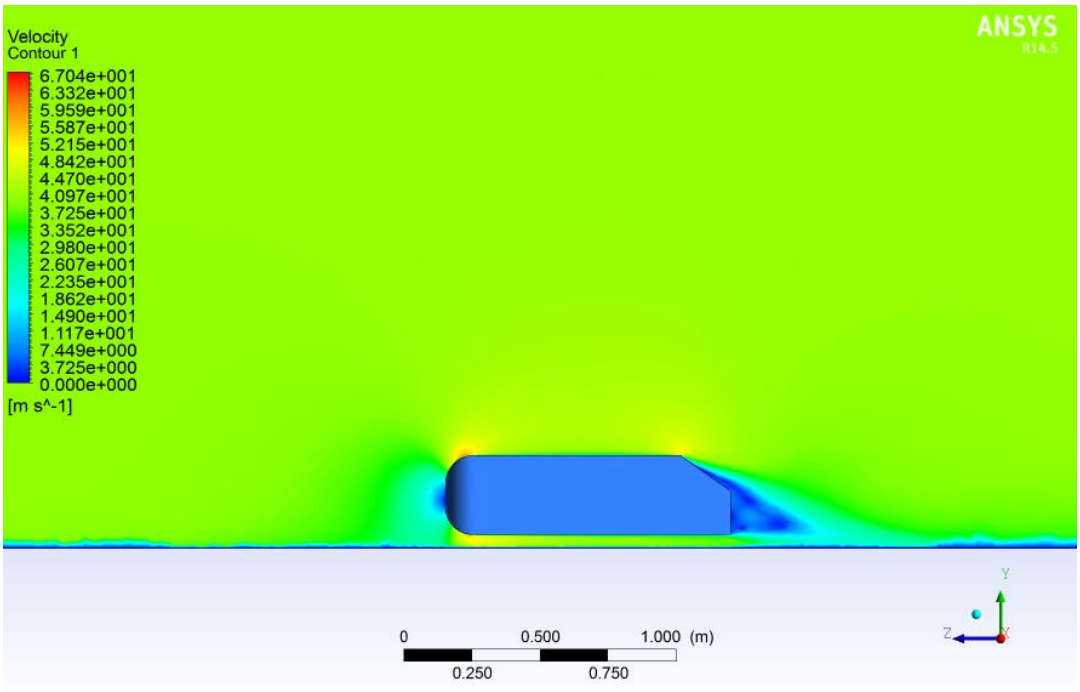

Fig. 6.2 Velocity Contour of the Ahmed body

In the velocity contour shown in the figure 6.2,the blue area is the wake behind the car.

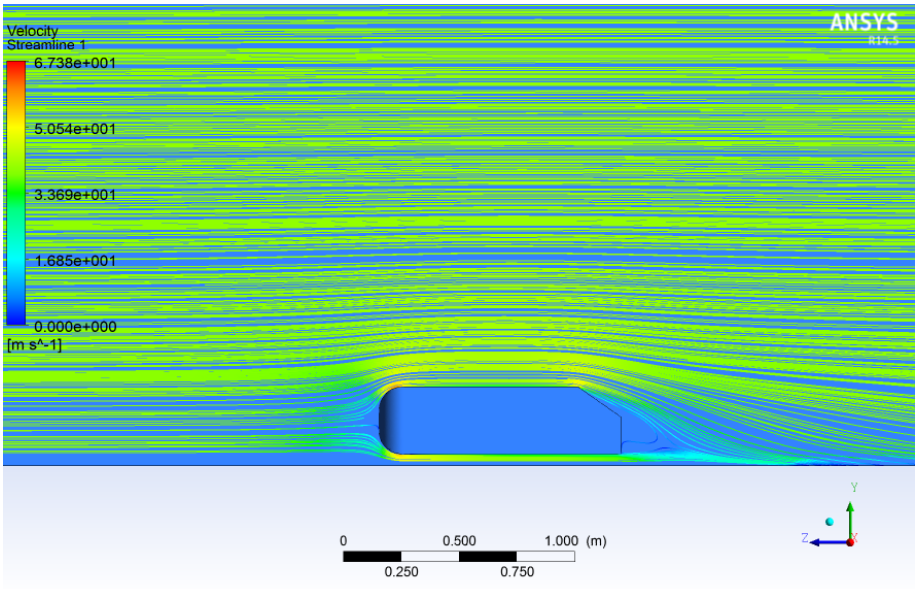

Fig. 6.3 Velocity Streamlines over the Ahmed Body

The streamlines clearly show recirculation behind the car which means that a wake has been formed.

(ii)With the brake plate at the rear of the car

With the brake plate behind the car, a drag coefficient of 0.351 was obtained .This represents an increase in the drag coefficient which represents an increase of 34% in the drag coefficient.

The velocity and pressure contours are shown in Fig.6.4 and Fig.6.6. respectively.

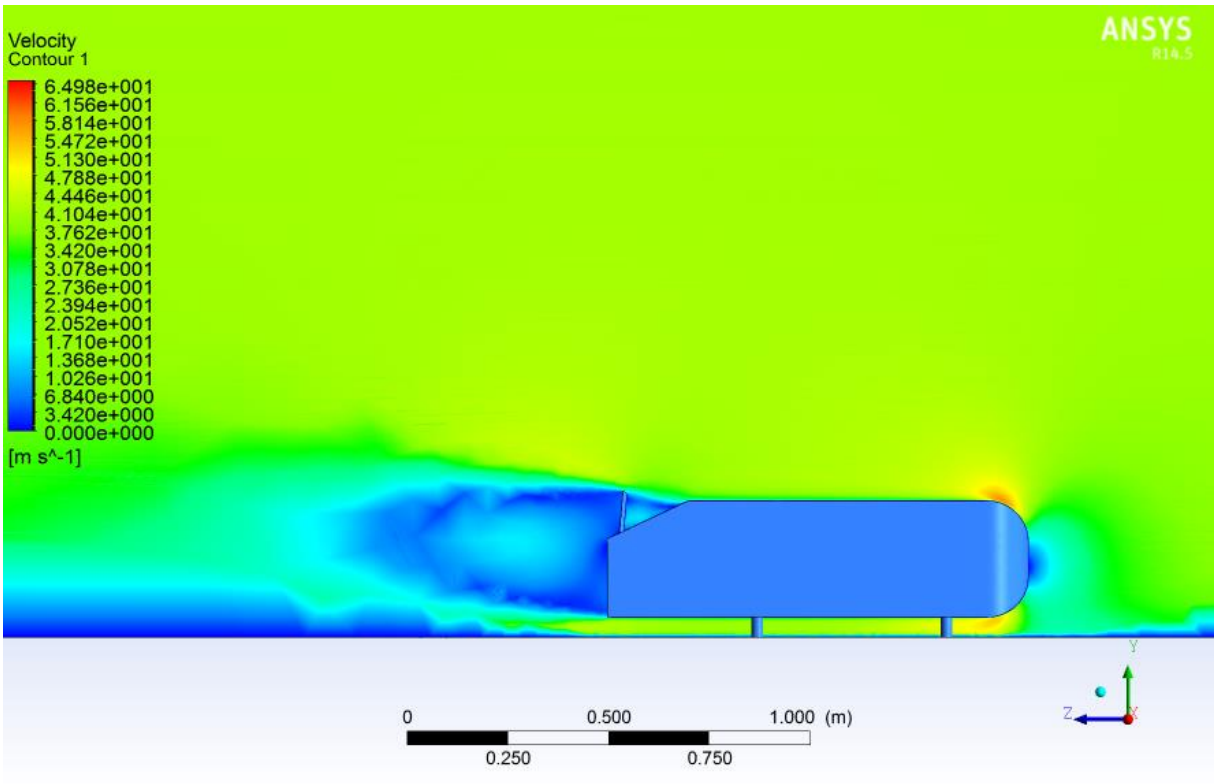

Fig.6.4 Velocity contour of the Ahmed body with rear Brake plate

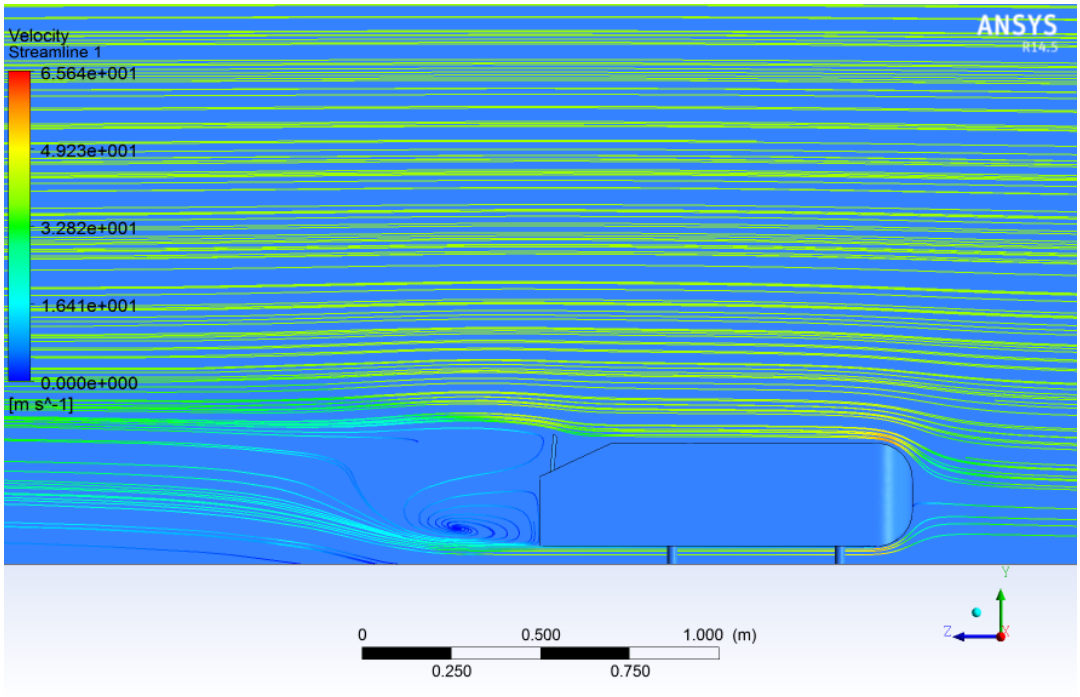

Fig. 6.5 Velocity Streamlines over the Ahmed body with rear Brake plate

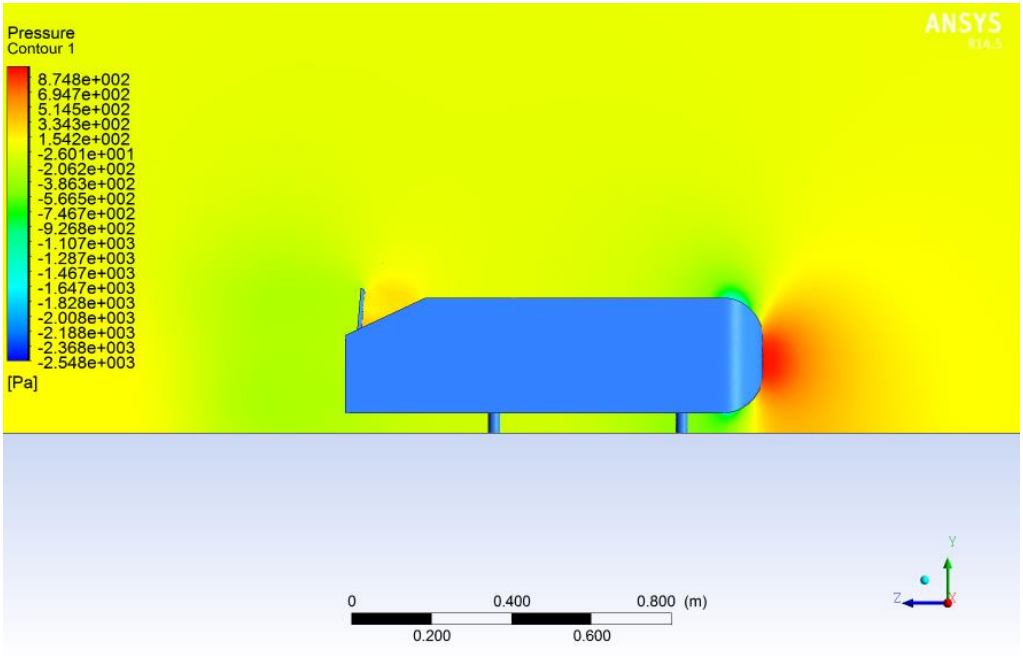

Fig. 6.6 Pressure contour of the Ahmed body with rear Brake plate

The velocity contours and streamlines show a formation of wake behind the vehicle. It can also be observed that the wake is larger than in the case without any brake plate.

(iii)It is implicitly understood that the maximum drag coefficient will be observed when the plate is exactly perpendicular to the flow direction .But due to excessive bending

moment when perpendicular and due to actuation constraints when perpendicular, 55^0 was chosen as the angle of inclination.

The height was fixed at 70mm and the position of the brake was varied. The position vs. drag coefficient drag obtained was as follows.

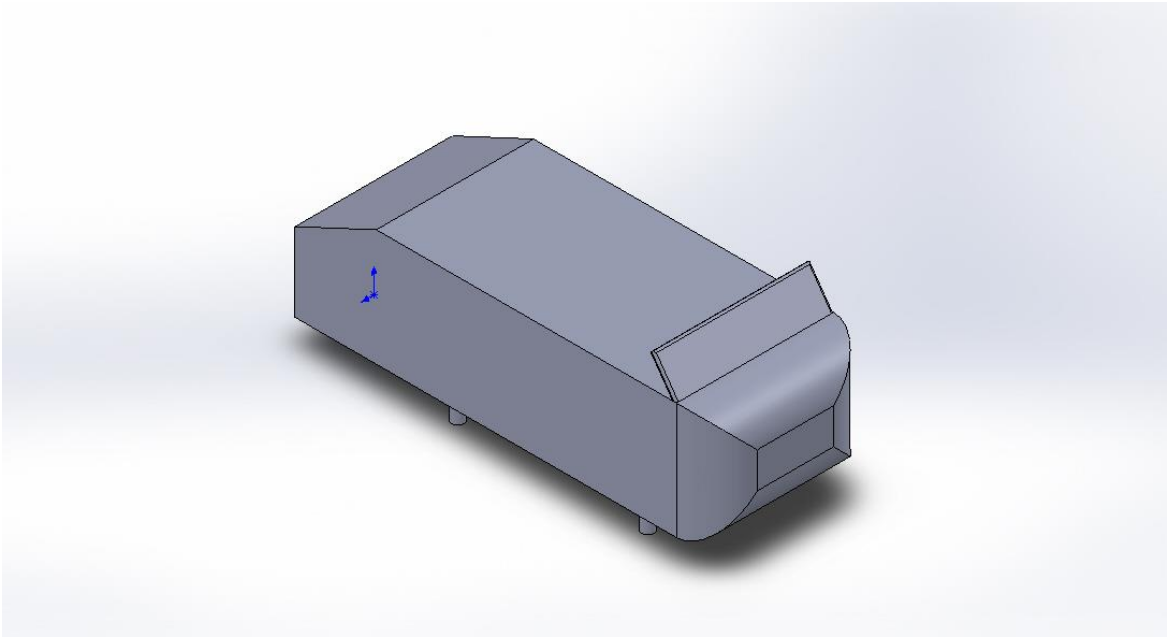

Fig.6.7.CAD model of the Ahmed body with the brake

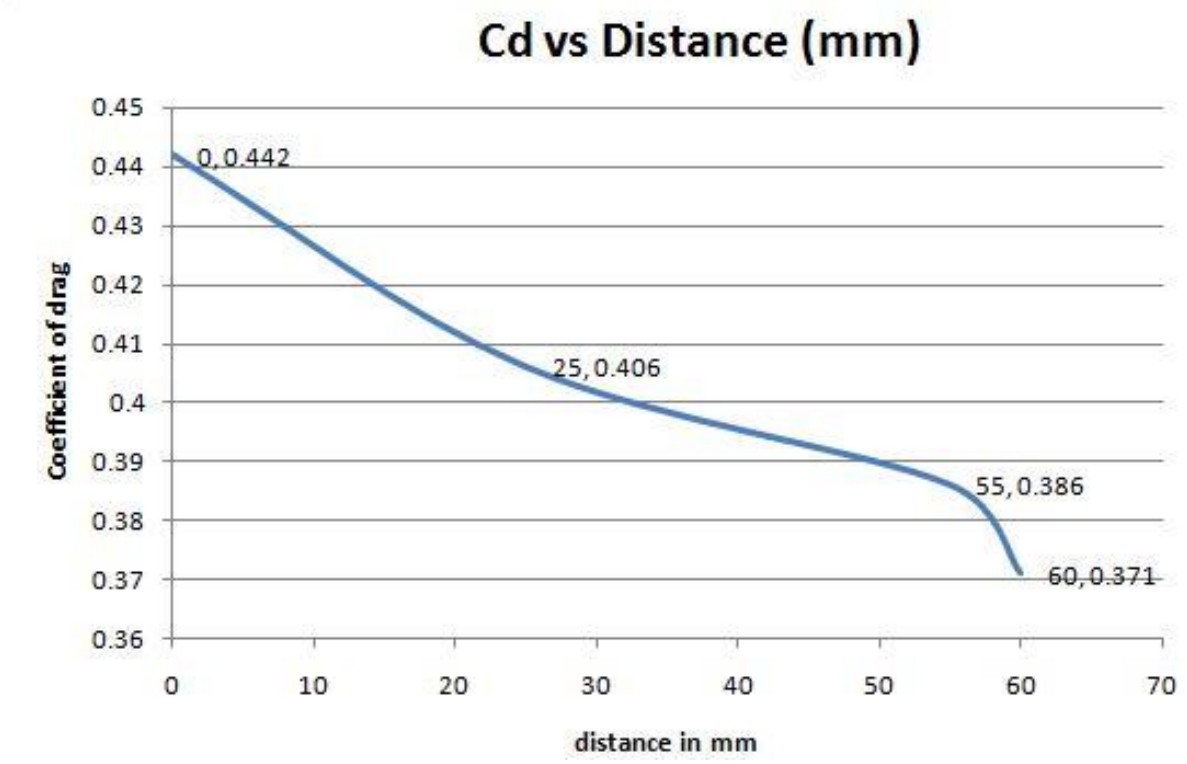

Fig.6.8. Coefficient of Drag –C_d vs. Distance

The height was then fixed at 100mm.The results obtained were more or less the same. Since there is very less increase in coefficient of drag with increase in height, the height was fixed at 70 mm.

The velocity and pressure contours over the Ahmed body with the brake as shown.

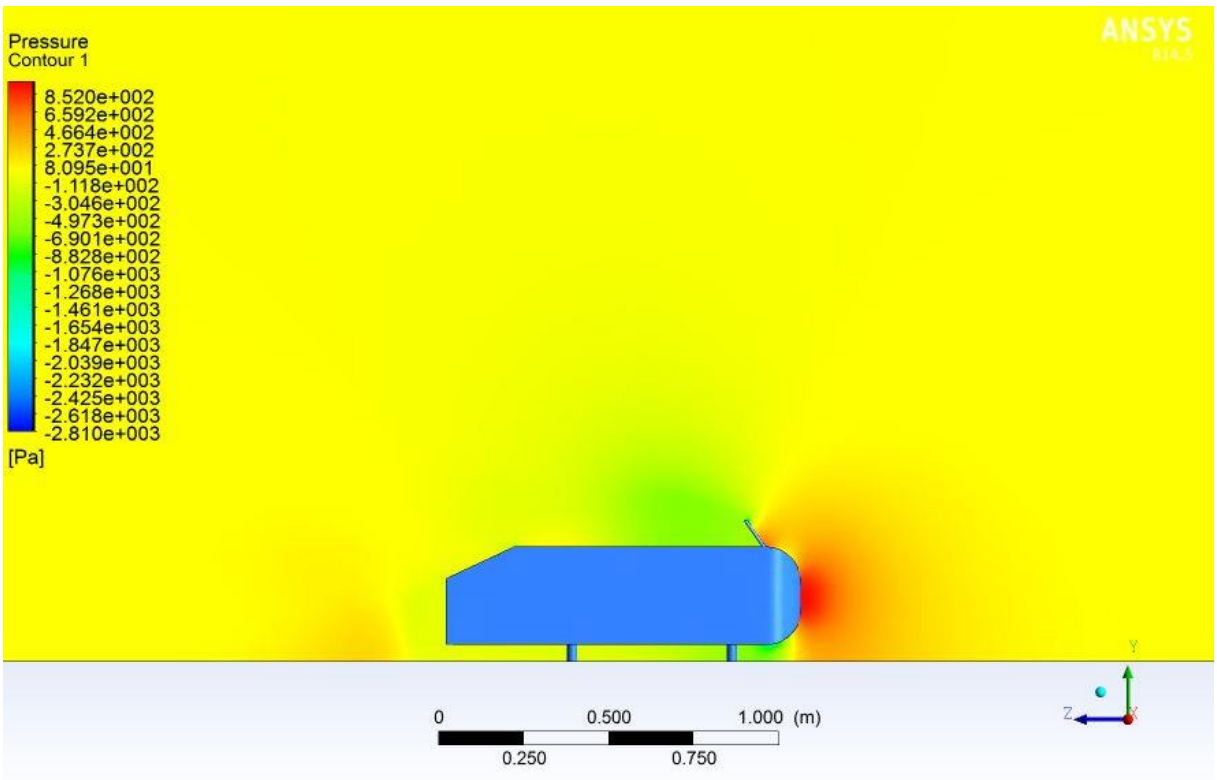

Fig.6.9 Pressure contour of the Ahmed Body with Front Brake plate

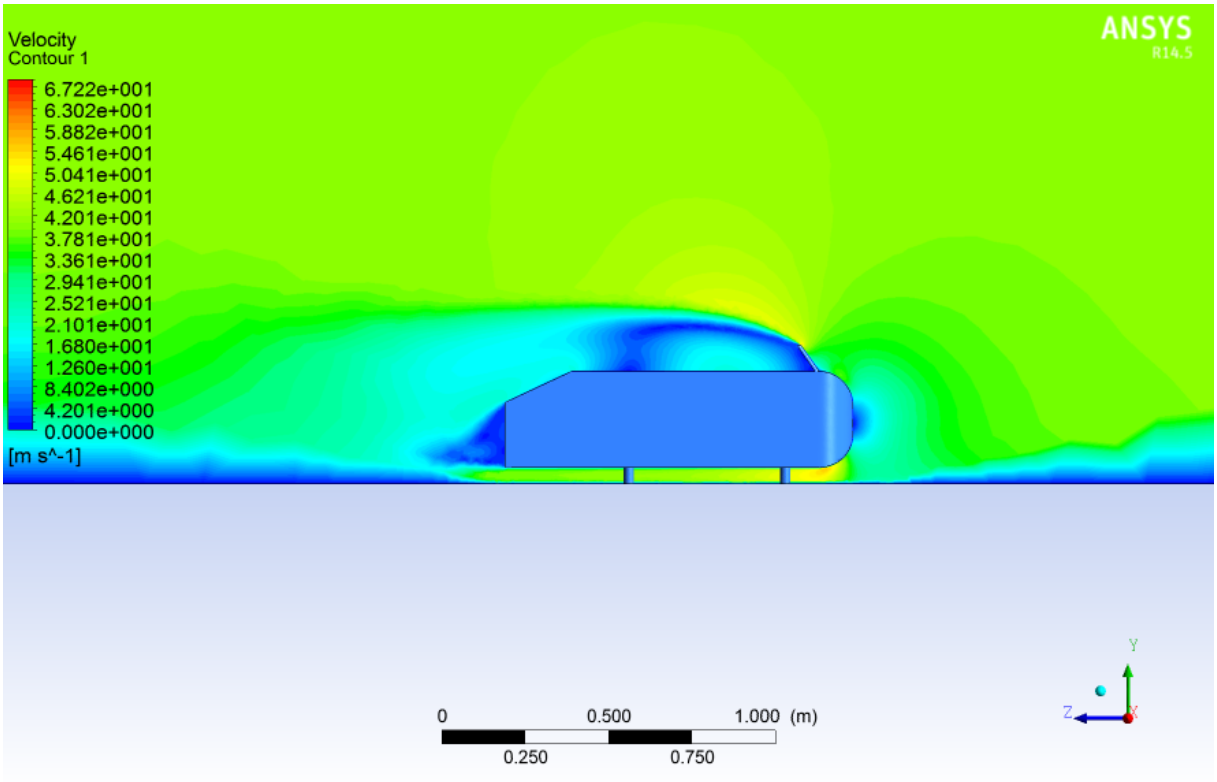

Fig.6.10 Velocity contour of the Ahmed Body with Front Brake plate

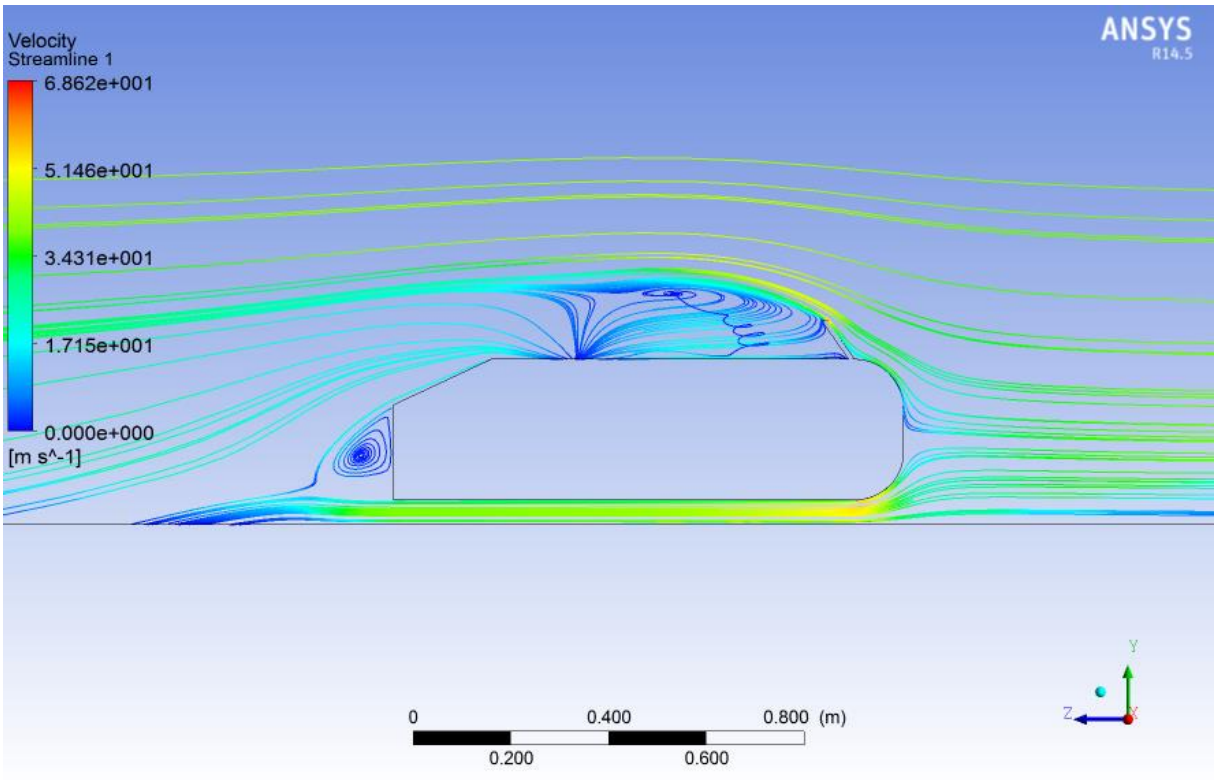

Fig.6.11 Velocity streamlines of the Ahmed Body with Front Brake plate

The figures 6.10 and 6.11 clearly show boundary layer separation just after the streamlines pass over the brake plate. The wake formed here is larger than the previous two cases of Ahmed body without the brake plate and the one with the brake at the rear.

6.3 Wind Tunnel testing

Parameters:

Velocity of test section: 160 kmph (44.44 m/s)

Length of test subject: 200 mm

Kinematic viscosity of air: $15.68*10^{-6}$ m^2/sec

Reynolds Number: 566836.733

Drag Calculations:

Angle of inclination of multi-tube manometer=45^o

Table 6.2 Manometer readings without Front Brake plate

Segment	Manometer reading(cm of water)	Pressure (Pascal)	Segmented areas(cm^2)
I	10	6912	4125
II	6	4147.2	3833.3
III	6	4147.2	3833.3
IV	7	4832.4	3833.3
V	9	6220.8	3000
VI	9	6220.8	3000

Table 6.3 Manometer readings without Front Brake plate

Segment	Manometer reading(cm of water)	Pressure (Pascal)	Segmented Areas(cm^2)
I	10.5	6048	4125
II	10.5	6048	112.5
III	6.5	3744	112.5
IV	7.5	4320	112.5
V	7.5	4320	3000
VI	3	1728	3000

Each centimeter head of water corresponds to 10 Pascal pressure. Since the manometers are inclined at an angle of 45^o, 1 m head of water corresponds to 7.07 Pascal pressure.

Net force in the x-direction= $F_x = \sum P_{xi} * S_{xi}$……1

Where P_{hi} is the pressure acting at i^t segment and six is the normal area where the pressure is acting.

Force in x-direction with brake=0.507 N

Force in x-direction without brake=0.4036

Frontal area for body without brake=4125 cm^2

Frontal area for body with brake=4237.5 cm^2

$$C_D = \frac{2F_d}{\rho v^2 A}$$ ……..2

Where

C_D is coefficient of Drag

F_{ad} is force due to drag

V is velocity of attack

A is projected Area

Coefficient of drag for body without brake=0.31

Coefficient of drag for body with brake=0.55

Percentage increase in C_D =66.66%

6.4. Test for effectiveness on a road car

Table 6.4 Variation of drag force on a road vehicle

Speed(kmph)	Drag Force without brake (N)	Drag force with brake (N)
160	671.6	1698.7
165	714.23	1806
170	758	1917
175	803	2032
180	850	2150
185	897	2271
200	1102	2788
220	1269	3211
230	1387	3110
240	1511	3822
250	1639	4147

Coefficient of drag of the 2D car model without brake: 0.31

Coefficient of drag of the 2D car model with brake: 0.51

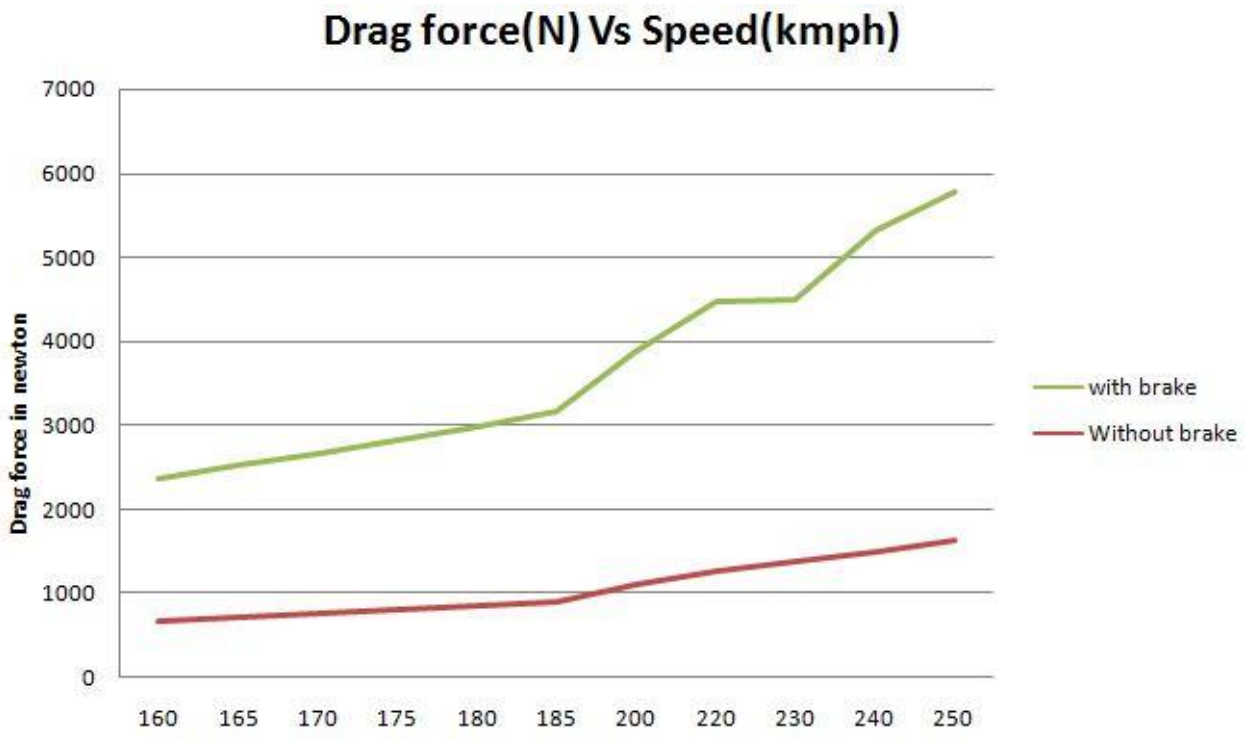

Fig. 6.12 Graph showing the variation of Drag Force (Newton) vs. Speed (Kmph)

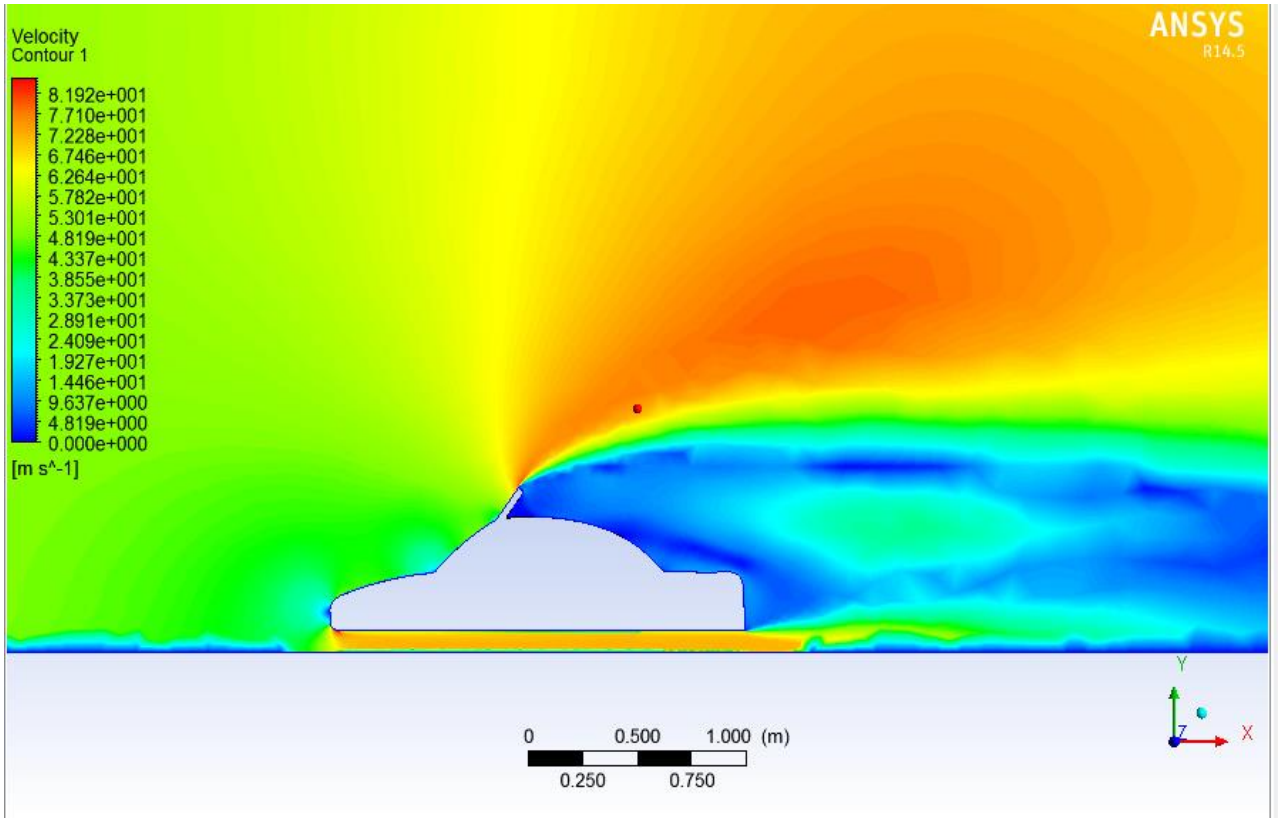

Fig. 6.13. Velocity contour for flow over car model with the brake

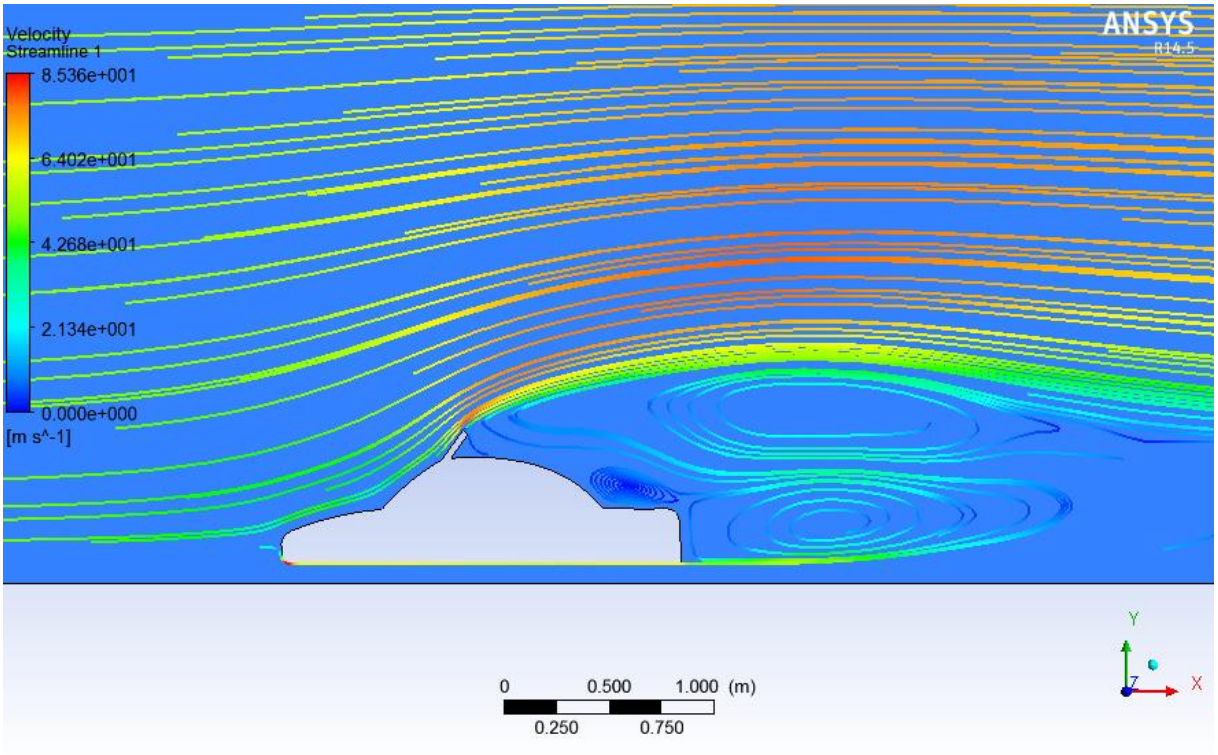

Fig. 6.14. Streamlines over the car body with the brake

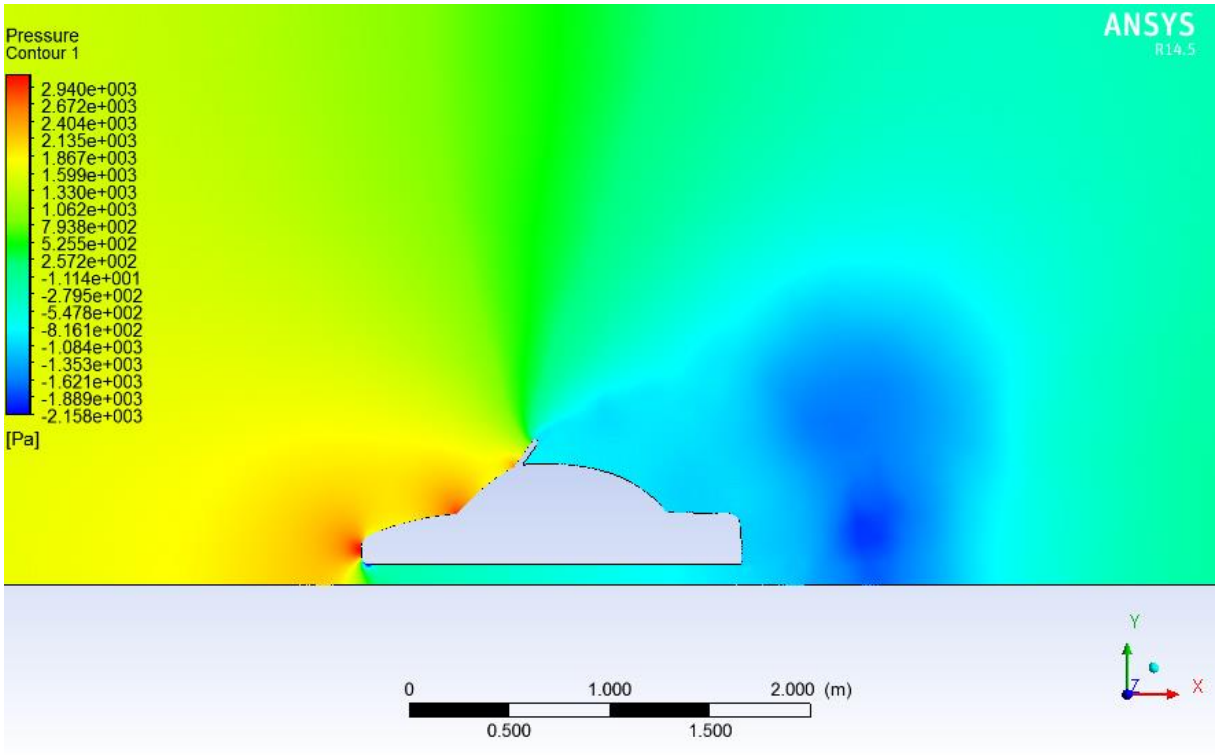

Fig. 6.15. Pressure contour for the flow over the car body with brake

CHAPTER 7

CONCLUSIONS

The studies on Ahmed body indicate an increase in the size of wake formed behind the Ahmed body. Speaking quantitatively, a 70% increase in coefficient of drag was observed. It can be concluded that the brake has worked as expected.

Further, when compared to a rear aerodynamic brake, a front aerodynamic brake is more effective. This justifies the use of the front aerodynamic brake over a rear aerodynamic brake.

Observing the results of the simulation of the brake on a road car, the drag force has accounted for more than 12% of the retarding force. This increase in drag force has reduced the braking distance for a speed of 160 kmph, the braking distance has reduced by 30%.This 30% decrease could prove to be the difference between life and death.

Also, due to increase in drag forces which are comparable to the reading forces due to mechanical braking, the load on the brake discs reduces, thus reducing the chance of brake disc failure.

Further, since the braking force is independent of the grip between the tires and the road, the brake will still be effective on wet surface. Even, in the case of hydroplaning-the loss of grip due to wet roads, the brake will still work.[22]

There is lot of turbulence produced behind the car. The same turbulent air flows over the vehicle behind. This turbulent air is detrimental to the aerodynamic performance of a streamlined body by increasing the skin friction drag. In racing applications, these phenomena can give a performance advantage.[23]

CHAPTER 8
FUTURE SCOPE

Further, the same brake plate can be extended to trains. Due to expected re-attachment of flow in a train, multiple plates can be used for more drag force while braking.

With decreasing reaction times of actuators, the effectiveness can be increased.

Due to unavailable computational resources, proper variation of coefficient of drag could not be observed. With proper computational resource, this task can be carried in order to have a better justification of using the brake.

REFERENCES

1.Web Link:http://www.autoevolution.com/news/braking-systems-history-6933.html

2.Web Link:http://abauto.net/auto-brake-service-and-brake-repair

3. Web Link:http://www.roadandtrack.com/the_road_ahead/evolution-of-brakes\

4. Web Link:http://www.autoevolution.com/news/brutally-reducing-all-kinetic-energy-the-romantic-high-tech-brake-guide-15189.html

5. eFunda, Inc."*Rapid Prototyping: An Overview*".Web Link: www.Efunda.com 2013-06-14.

6.Web Link: http://www.formula1-dictionary.net/rapid_prototyping.html

7.Web Link: http://www.ielm.ust.hk/dfaculty/ajay/courses/ieem513/RP/RPlec.html

8.Web Link:http://en.wikipedia.org/wiki/Fused_deposition_modeling

9.Web Link: http://www.formula1-dictionary.net/wind_tunnel.html

10.Web Link:https://www.grc.nasa.gov/www/k-12/airplane/tunoret.html

11. Tony Saad. "*Turbulence modeling for beginners"* pp 3-5

12. Web Link:http://en.wikipedia.org/wiki/K-epsilon_turbulence_model

13.Osama Abdul Ghani."*Design optimization of aerodynamic drag at the rear of generic passenger cars using NURBS representation*"

14.Cooper, K. R. "*Bluff body aerodynamics as applied to vehicles"* Journal of Wind Engineering and Industrial Aerodynamics, 49, pp. 1-22. (1993)

15. S. R. Ahmed, G. Ramm, and G. Faltin. "*Some salient features of the time averaged ground vehicle wake"* SAE Paper 840300. (1984)

16. Morelli, A. "*A New Aerodynamic Approach to Advanced Automobile Basic Shapes*" SAE Technical Paper 2000-01-0491.(2000)

17. Hucho, W. H., & Sovran, G."*Aerodynamics of road vehicles*"

Annual review of fluid mechanics.25(1), pp 485-537. (1993)

18.Bayraktar, I., Landman, D., and Baysal, O. "*Experimental and Computational Investigation of Ahmed Body for Ground Vehicle Aerodynamics"* SAE Technical Paper 2001-01-2742. (2001)

19. SoumyaKanta Das1, Pavan Kumar2 and ShwetaRawat3 "*Alterations of Formula 3 Race Car Diffuser Geometry forOptimizedDownforce"*

20.NASA/TP—1998–208396*"Application of Rapid Prototyping Methodsto High-Speed Wind Tunnel Testing"*

21.Web Link:http://en.wikipedia.org/wiki/Actuator

22 Web Link: http://en.wikipedia.org/wiki/Aquaplaning

23. Ascher H. Shapiro, Shape and Flow - The fluid dynamics of drag, Anchor Books, 1961